THE FATE OF NITROGEN POLLUTION IN HIGH-LATITUDE WINTER:

INVESTIGATIONS USING A 1-D PHOTOCHEMICAL *MODEL*

By

Patrick L. Joyce

RECOMMENDED:

Catherine F. Cahill

Advisory Committee Chair

Chair, Department of Chemistry and Biochemistry

APPROVED:

Dean, College of Natural Science and Mathematics

Dean of the Graduate School

Dec 6, 2011

Date

THE FATE OF NITROGEN POLLUTION IN HIGH-LATITUDE WINTER: INVESTIGATIONS USING A 1-D PHOTOCHEMICAL MODEL

A

THESIS

Presented to the Faculty

of the University of Alaska Fairbanks

in Partial Fulfillment of the Requirements

for the Degree of

MASTER OF SCIENCE

By

Patrick L. Joyce, B.S.

Fairbanks, Alaska

December 2011

Abstract

Simulations using a 1-D photochemical model were performed to analyze the fate of NO_x pollution in a high-latitude winter environment. Modeled pollution emissions were constrained by observations from downtown Fairbanks and the model reproduced dilution of NO_x on timescales in agreement with field measurements on the edge and outside of the urban area of Fairbanks. The model was updated from previous versions to include calculations of reactions of N_2O_5 on aerosol particles and an empirically-derived value for dry deposition velocity of N_2O_5 to the snowpack, which acts as a competing loss of N_2O_5. It was found that dry deposition of N_2O_5 causes a significant fraction of N_2O_5 loss near the snowpack, but reactions on aerosol particles dominate loss of N_2O_5 over the total atmospheric column. Sensitivity experiment results indicate a strong sensitivity to urban area density (affecting NO flux), season and clouds (affecting photolysis), and weather and climate (affecting temperature), implying a strong sensitivity of the results to urban planning and climate change. Model simulations produced large amounts of secondary ammonium nitrate downwind of the polluted area due to NO_x oxidation and subsequent reactions with ammonia on aerosol particles.

Table of Contents

Page

List of Figures

Page

List of Tables

Page

Acknowledgments

I would like to thank my advisor, Bill Simpson, for all of his guidance through this project. With a door that was always open, willingness to help, a genuine care for his students, and an answer for every question, one couldn't ask for a better advisor.

I would like to thank Roland von Glasow in Norwich, UK for his time and energy spent teaching me about MISTRA. It was a pleasure to spend my time in Norwich learning the ropes. From command line basics to heterogeneous reaction parameterizations, he was always had the answer and could always point me to the correct sub-routine. A big thanks to my committee members, Catherine Cahill and Tom Trainor for their revisions, comments, and suggestions which have strengthened this thesis and manuscript for submission to publication.

I would like to thank my parents for their never ending support and caring. Without their teachings from an early age I never would have the curiosity about the physical world which has led me to research. Without their support all along my educational path I would not have been able to obtain an advanced degree.

I would like to acknowledge the National Oceanic and Atmospheric Administration (NOAA) for use of the Ferret program for analysis of model output and the University Corporation for Atmospheric Research (UCAR) for the use of NCAR Command Language (NCL) plotting software, which was used to generate the figures in this thesis. I would like to extend sincere thanks to Paula Moreira for her assistance with NCL plots.

Lastly, thanks to the National Science Foundation (NSF). This project was funded by NSF under grant ATM-0926220.

Chapter 1: Introduction

1.1 Motivation

Anthropogenic activities such as fuel combustion and power generation are carried out at extremely high temperatures and produce chemical byproducts that are emitted into the atmosphere. The chemical species nitric oxide (NO) is emitted when naturally occurring N_2 and O_2 react to form 2NO under these high temperature conditions. Nitric oxide rapidly reacts with background O_3 to form nitrogen dioxide (NO_2), and together NO and NO_2 form the chemical family known as NO_x. Typically, >90% of NO_x emitted is in the form of NO (Finlayson-Pitts and Pitts, 2000).

Once in the atmosphere, NO_x reacts through oxidation pathways that are dependent on temperature, sunlight, and other reactive gases in the air parcel. Through such oxidation pathways, NO_x emissions ultimately end up in the form of nitric acid (HNO_3). Nitric acid can exist in the gas phase or can be present in atmospheric aerosol particles as nitrate (NO_3^-). Aerosol particles can remain suspended in the atmosphere or deposit to surfaces such as the ground or foliage. Deposited nitrogen species can fertilize soil where nitrogen is considered to be the growth-limiting nutrient for vegetation and acidic species such as HNO_3 can contribute to acidification of groundwater (Driscoll et al., 2001). Stevens et al. (2004) have shown that increased nitrogen deposition led to a linear reduction of grassland species across Great Britain. Physical deformations of ponderosa pine and California black oak trees have been found after exposure to high concentrations of nitric acid (Bytnerowicz et al., 1998). Fenn et al. (2003) have shown

that some aquatic and terrestrial plant and microbial communities are significantly altered by nitrogen deposition at rates as low as 3-8 kg nitrogen per hectare per yr.

Empirical observations suggest Alaska may receive increased nitrogen deposition when compared to other high-latitude environments due to anthropogenic activities. Jaffe and Zukowski (1993) measured nitrate levels in snow samples between Fairbanks (64.76°N) and Deadhorse (71.29°N) and found concentrations to be 1.5 times higher than those observed in Greenland. Additionally, a gradient with latitude was found, with nitrate concentrations increasing as observation sites moved north towards the substantial source of NO_x emissions in Prudhoe Bay on the Arctic coast. Jaffe and Zukowski's study shows the snowpack in interior Alaska is under a greater influence from anthropogenic constituents than other remote sites in the Northern Hemisphere.

Currently, the comprehensive fate of emitted nitrogen in Alaska is unknown. Studies by the Simpson group (Ayers et al., 2005; Ayers and Simpson, 2006) have focused on the measurement of an intermediate species in NO_x oxidation called dinitrogen pentoxide (N_2O_5), which can exist in high abundance under dark, winter conditions. Additional studies by our group have analyzed loss processes of N_2O_5 (Apodaca et al., 2008) and measured deposition rates to the snowpack (Huff et al., 2011).

1.2 Background

Nighttime emissions of NO are oxidized at night through the following reactions known as the "dark" oxidation pathway:

$$NO + O_3 \longrightarrow NO_2 + O_2 \quad \text{(R1)}$$

$$NO_2 + O_3 \longrightarrow NO_3 + O_2 \quad \text{(R2)}$$

$$NO_2 + NO_3 + M \underset{\leftarrow}{\longrightarrow} N_2O_5 + M \quad \text{(R3)}$$

$$N_2O_5 + H_2O \xrightarrow{surface} 2HNO_3 \quad \text{(R4)}$$

In the absence of photolysis, ozone is not produced and can be depleted through reactions (R1) and (R2). Reaction (R3) is a thermodynamic equilibrium where cold temperatures favor formation of N_2O_5. Lack of photolysis allows the nitrate radical (NO_3) to accumulate and subsequently react to form N_2O_5. Reaction (R4) is the process known as "heterogeneous hydrolysis" and occurs when a gas phase N_2O_5 molecule reacts with water on a surface such as an aerosol particle, the ground, snowpack, or foliage.

In contrast, the main oxidation pathway during the day is controlled by hydroxyl radical, OH:

$$NO_2 + OH \rightarrow HNO_3 \quad \text{(R5)}$$

At mid latitudes and warm temperatures, reaction (R5) is the dominant NO_x oxidation pathway. At high latitudes, however, 80% of NO_x is lost through the dark oxidation pathway in winter (Dentener and Crutzen, 1993).

Figure 1.1 outlines competing pathways for reaction (R4) by aerosol and surface deposition. The aerosol surface reactivity in reaction (R4) is accounted for through the reactive uptake coefficient, γ. Reactive uptake is dependent on aerosol surface area,

where increased aerosol surface area allows for more molecular collisions on the surface where a reaction can occur. The competing mechanism for reaction (R4) is "dry deposition" to the snowpack, where the same process can occur on the ground. This reaction rate to the snowpack is controlled by the dry deposition velocity, v_{dep}, typically measured in cm s^{-1}.

Chemical lifetime, τ, is a useful way to quantify residence time and reactivity of an atmospheric constituent:

$$\tau = \frac{1}{k} \tag{1.1}$$

where k is the loss rate. Typical mid-latitude lifetimes of NO_x are on the order of 1 day, but at high latitudes may be shorter or longer due to extreme environmental conditions.

1.3 Field measurements of nocturnal nitrogen species

Nocturnal mixing ratios of nitrogen species such as N_2O_5, NO_3, and NO_x have been measured extensively at mid latitudes. Despite relatively warm temperatures at mid latitudes, the nighttime oxidation pathway can still be extremely significant. Measurements east of San Francisco Bay in California found total HNO_3 abundance produced by N_2O_5 hydrolysis during the night was comparable to ambient NO_2 abundance, and was estimated to be a factor of nine larger than HNO_3 produced during the day (Wood et al., 2005). In a high-latitude winter environment with long nights and cold temperatures, the dark oxidation pathway is likely intensified. Ayers and Simpson

(2006) first measured N_2O_5 at high latitudes and found that formation of NO_3 though reaction (R2) was likely the limiting step in NO_x oxidation. Upon formation in cold temperatures, NO_3 rapidly reacts with NO_2 to form N_2O_5 through reaction (R3), which then reacts through reaction (R4) in a matter of minutes. At warm temperatures, N_2O_5 can thermally dissociate through the back reaction of (R3), but this is not observed in temperatures below 273 K.

Ice surfaces were found to be a likely key loss mechanism of N_2O_5 by Apodaca et al. (2008). They determined that lifetimes of N_2O_5 where shorter in ice-saturated air masses (~6 min) than in air masses sub-saturated with respect to ice (~20 min). Additionally, vertical gradients in N_2O_5 have been measured by aircraft (Brown et al., 2007b) and in higher resolution directly from the surface using a 300 m tower (Brown et al., 2007a). Results from these studies have shown distinct differences in reactivity with altitude, where N_2O_5 can serve as a sink of NO_x and O_3 near the surface but as a reservoir aloft. This suggests that the large surface area of snowpack on the ground can cause a significant loss of N_2O_5. In addition to existing as gas phase N_2O_5 aloft, HNO_3 formed in aerosols through reaction (R4) can undergo long range transport.

The evidence of different chemical regimes of N_2O_5 based on altitude has raised the question of relative loss rates from aerosol reactivity versus dry deposition of N_2O_5. Stutz et al. (2004) showed that chemistry in nitrogen polluted areas is most strongly altitude dependent in the first 100 m of the atmosphere. This suggests reactions on or near the surface play a key role in NO_x oxidation and N_2O_5 removal. To quantify the loss rate to the snowpack, we measured the dry deposition velocity of N_2O_5 to be 0.59 ± 0.47 cm s^{-1}

(Huff et al., 2011) in a winter, sub-Arctic environment. These were the first known measurements of their kind. Huff (2010) also measured longer lifetimes of N_2O_5 aloft from the roof of the Geophysical Institute in Fairbanks (85 m) than near the surface.

1.4 Reactive uptake of N_2O_5

Reactive uptake coefficient, γ, also known as "reaction probability" can be defined as the fraction of gas phase to aerosol particle collisions and result in a chemical reaction. For example, a γ of 0.2 means 20% of collisions between a gas-phase molecule and an aerosol particle resulted in a reaction and chemical transformation into the aerosol. Brown et al. (2006) measured reactive uptake of N_2O_5 (γ_{N2O5}) on sub-micron aerosols as:

$$\gamma_{N_2O_5} = \frac{4k_{N_2O_5}}{c_{mean}A} \tag{1.3}$$

where $k_{N_2O_5}$ is the first-order loss rate of N_2O_5 by reaction (R4) on aerosols, c_{mean} is the mean molecular speed of the N_2O_5 particle, and A is the aerosol surface area density. For the purposes of this thesis, $\gamma = \gamma_{N_2O_5}$.

In addition to dependence on aerosol surface area, it is well documented in laboratory studies that γ can be significantly affected by aerosol composition and relative humidity (Mozurkewich and Calvert, 1988; Hanson and Ravishankara, 1991; Van Doren et al., 1991; Hanson, 1997; Hu and Abbatt, 1997). It has also been found that sufficient amounts of NO_3^- in a particle can hinder γ by the "nitrate effect" (Mentel et al., 1999),

where increased concentrations of NO_3^- hinder reactions of aqueous N_2O_5 upon uptake in the particle. Additionally, McNeill (2006) found that a mono-layer of sodium dodecyl sulfate reduced γ by a factor of 10. In this manner, organic layers on aerosol particles may "poison" aerosol reactivity.

An aircraft study conducted by Brown et al. (2006) over the northeast contiguous United States found γ was highly variable in the atmosphere and strongly dependent on aerosol composition. The study found that regions characterized by acidic aerosol composition due to high sulfate (SO_4^{2-}) concentrations resulted in higher values of γ. Regions considered neutralized as determined by a molar ratio of $NH_4^+/SO_4^{2-} \geq 2$ implying an aerosol composition of ammonium sulfate [$(NH_4)_2SO_4$] saw low values of γ and an increased abundance of N_2O_5 in the atmosphere.

Bertram and Thornton (2009) used laboratory data to parameterize γ's dependence on liquid water content ($H_2O_{(l)}$), NO_3^-, and chloride (Cl^-) in a variety of aerosol compositions as:

$$\gamma_{N_2O_5} = A(\beta - \beta e^{-\delta[H_2O]})\left(1 - \frac{1}{1 + \phi\frac{[H_2O]}{[NO_3^-]} + \xi\frac{[Cl^-]}{[NO_3^-]}}\right) \quad (1.3)$$

Parameters used in equation (1.3) can be found in Table 1.1. The β portion of the equation isolates the effect of H_2O on γ and the parameters ϕ and ξ are ratios of rate

coefficients of competing reactions for the species in the numerator and denominator of the corresponding term. Bertram and Thornton confirmed that nitrate can suppress γ when the molar ratio of $H_2O/NO_3^- < 20$. Additionally, it was found that trace amounts of Cl^- can negate the nitrate effect when the molar ratio of $Cl^-/NO_3^- > 0.1$.

1.5 Chlorine activation by N_2O_5

In addition to affecting γ, Cl^- in a particle can react with N_2O_5 to form nitryl chloride ($ClNO_2$) though the reaction first presented by Graedel and Keene (1995) and refined by Thornton et al. (2010):

$$N_2O_{5(g)} + Cl^-_{(aq)} \xrightarrow{surface} ClNO_{2(g)} + NO_3^-{}_{(aq)} \quad \text{(R6)}$$

Chlorine activation occurs when an ionic chloride (Cl^-) reacts to form a chlorine radical (Cl) in the atmosphere. In sufficient sunlight $ClNO_2$ can undergo photolysis, which releases Cl radical and reforms NO_x:

$$ClNO_2 + h\nu \rightarrow Cl + NO_2 \quad \text{(R7)}$$

Chlorine radical in the atmosphere is extremely reactive and photochemically active halogen compounds can lead to removal of hydrocarbon species (Jobson et al., 1994) and influence destruction of ozone at ground level in polar spring (Finlayson-Pitts and Pitts, 2000). Nitryl chloride is typically observed near coastlines due to high concentrations of

Cl^- in maritime aerosol (Osthoff et al., 2008). Through simultaneous measurements of N_2O_5 and $ClNO_2$, Osthoff et al. (2008) showed that reaction (R6) occurring at night was the main formation pathway of $ClNO_2$. They also determined from measured $ClNO_2$ abundances and photolysis rates that the resulting Cl radical source can approach $1x10^6$ atoms cm^{-3} s^{-1}.

Thornton et al. (2010) measured a similar strong correlation between $ClNO_2$ and N_2O_5 in Boulder, Colorado and showed that measured Cl^- in the particles was not enough to account for $ClNO_2$ observations. For the mechanism presented as a mid-continental chlorine source, gaseous equilibrium with hydrogen chloride (HCl) was assumed to be the Cl^- source for reaction (R6) and was calculated using thermodynamic models constrained by measurements. Using the GEOS-Chem global chemical model, Thornton et al. found the Cl radical production rate to be 2 to 6 times higher than original estimates due to the $ClNO_2$ source.

1.6 Dry deposition

Formulating the process of a gaseous species coming in contact with a surface and undergoing a chemical reaction can be complex. In order for a gaseous molecule to reach the ground surface, it must overcome resistance to travel through the atmosphere, resistance from the deposition surface itself, and chemical dissociation upon contact with water. To account for these processes, v_{dep} is defined as the sum of resistances in a series, similar to that of an electrical circuit:

$$v_{dep} = \frac{1}{r_a + r_b + r_c} \tag{1.4}$$

where r_a is aerodynamic resistance, r_b is quasi-laminar resistance, and r_c is surface resistance (Seinfeld and Pandis, 2000). Aerodynamic resistance is the same for all gases, while quasi-laminar and surface resistances are species dependent. Quasi-laminar resistance depends on the molecular diffusivity of the gas and accounts for a viscous boundary layer adjacent to the surface on which deposition is occurring (Seinfeld and Pandis, 2006). Surface resistance is a sum of vegetative, lower canopy, and ground resistance acting in parallel. A parameterization for r_c can be applied to 11 different land use types under five different seasonal categories (Wesely, 1989; Wesely and Hicks, 2000). Included also is a dependence on Henry's Law coefficients for each gaseous species and correction factors for species such as SO_2, HNO_3, and NH_3 which dissociate upon absorption into water, which is often acts as the deposition surface. Modeled values of dry deposition by the Wesely or similar methods have been used extensively in global transport models (Hough, 1991; Kanakidou et al., 1991; Hauglustaine et al., 1994).

Measurements of v_{dep} of nocturnal nitrogen species, however, are scarce due to difficult flux measurements. Upward vertical fluxes of NO_x have been measured in Greenland, but were found to be highly correlated with diurnal variations in sunlight (Honrath et al., 2002) and suggest a photolytic release of NO_2 from the snowpack. Wesely and Hicks (2000) state that due to low solubility and low oxidizing capacity, NO dry deposition is usually negligible, while NO_2 dry deposition velocities are similar to those of O_3. For comparison, Hauglustaine (1994) presented modeled dry deposition

velocities over ice and snow to be 0.002, 0.01, and 0.5 cm s^{-1} for NO, NO_2 and HNO_3, respectively. In Huff et al. (2011) we presented the first measured value of v_{dep} of N_2O_5 over snowpack in a sub-Arctic environment to be 0.59 cm s^{-1}. In this experiment, chemical fluxes of N_2O_5 were measured using cavity ring-down spectroscopy (CRDS) with a movable chemical inlet and v_{dep} of N_2O_5 calculated via the flux using the aerodynamic gradient method (Huff, 2010).

1.7 Previous modeling studies of nocturnal nitrogen oxidation

Modeling work on nocturnal nitrogen oxidation is limited. In the most in-depth study of its kind, Geyer and Stutz (2004) modeled vertical profiles of NO_x, NO_3, N_2O_5, and O_3 and presented evidence that single altitude observations and single box models are not sufficient to characterize nocturnal nitrogen reactivity. They found strong negative vertical gradients of NO_2 that suggested NO_x removal primarily occurs in the upper nocturnal boundary layer. More importantly, Geyer and Stuz (2004) found the slow upward transport of NO from ground level and the simultaneous chemistry controlled the vertical structure of NO_x, NO_3, and N_2O_5. They also found that dry deposition of NO_2 and O_3, calculated explicitly by their model, were significant losses of NO_2 and O_3 and vertical transport of N_2O_5 played a key role in the vertical profile of N_2O_5. These vertical gradients led Geyer and Stutz to conclude that chemical steady state equations using NO_3 and N_2O_5 are not sufficient to describe the entire nocturnal boundary layer when vertical fluxes of N_2O_5 exist.

A later study by Sommariva et al. (2008) used ship-borne measurements of NO_3 and N_2O_5 off the Northeastern United States coast to constrain their model. These observations showed that that removal by fog droplets was the dominant N_2O_5 loss mechanism when fog was present, illustrating the importance of heterogeneous hydrolysis. Model results by Sommariva et al. (2008) overestimated NO_3 and N_2O_5 concentrations by 30-50%, but did find a weak dependence on nitrate aerosol composition. Work by Thornton et al. (2010) showed the fraction of NO_x removed via N_2O_5 is as high as 50% in regions of the Northeast US. To our knowledge, no model studies of nocturnal NO_x oxidation have been performed for high-latitude conditions. Fractions of NO_x lost by the nocturnal mechanism at high latitudes could be >50% and is cause for further study.

1.8 Estimations of nitrogen deposition near Fairbanks

Nitrogen deposition at a rate of 3-8 kg nitrogen ha^{-1} yr^{-1} (3.4-9.1 x 10^{-8} kg m^{-2} h^{-1}) has been found to have a significant impact on ecological systems (Fenn et al., 2003). Total emissions in the Fairbanks North Star Borough (FNSB) in 2005 were reported to be 10462 ton NO_x yr^{-1} (325.9 kg N hr^{-1}) (ADEC, 2008). A map of the area boundary of FNSB is included as Fig. 1.2. The largest point source in the area was the Golden Valley Electric Association North Pole Power Plant and made up 62% of total point sources of NO_x in the FNSB. Mobile sources make up 26.4% of total NO_x emissions reported for 2005 (ADEC, 2008).

As a first estimation experiment, it was assumed that all emitted NO_x followed the oxidation mechanism through reactions (R1) to (R4), with (R1), (R3), and (R4) occurring instantaneously in the forward direction. In order to estimate the surface area over which deposition occurs, the lifetime of NO_x to be destroyed by reaction (R2) must first be calculated. Figure 1.3 demonstrates the temperature dependence of the approximate lifetime of NO_x in the atmosphere based on reaction (R2). This reaction that forms NO_3 is strongly dependent on temperature and is the limiting step in the nocturnal nitrogen oxidation pathway.

For the purpose of this experiment, a source rate of 325.9 kg N hr^{-1} was located at the midpoint between Fairbanks and North Pole (Fig. 1.4). If all emissions are assumed to be deposited over the area of the FNSB boundary, a nitrogen deposition rate of $5.7x10^{-8}$ kg m^{-2} h^{-1} would result, a value deemed able to affect biota by Fenn et al. (2003). For a better approximation, it is assumed the plume drifts downwind from the defined point source with an average wind speed, direction, and temperature of 1.3 m s^{-1}, NNE, and 258 K, respectively (ACRC, 2010). Assuming a 45° angle of downwind dispersion from the point source, a 1.3 m s^{-1} wind speed results in a theoretical deposition area of 10,700 km^2 and a nitrogen deposition rate of $3.1x10^{-8}$ kg N hr^{-1}, a value just below the threshold as presented by Fenn et al. (2003).

Caveats regarding this experiment include the assumption the plume "dilutes" evenly over the downwind sector with the largest amount of area farthest away from the point source, due to the shape of the sector. In reality, increased concentrations near the point source would result in greater deposition rates near the source. Additionally,

heterogeneous processes are assumed to be instantaneous and entirely snowpack deposition. However, vertical mixing of the plume in the atmosphere cannot be accounted for with this approach. The above experiment illustrates the possibility of significant nitrogen deposition downwind of Fairbanks but clearly shows a more advanced technique is necessary.

1.9 Structure of thesis

This work begins by outlining the above background information regarding nocturnal nitrogen oxidation and related atmospheric processes in Chapter 1. Chapter 2 presents a simulation of the nocturnal NO_x plume emitted from Fairbanks, Alaska in the month of November using MISTRA, a 1-dimensional (1-D) microphysical chemical model (von Glasow et al., 2002). Analysis of the fate of emitted NO_x and sensitivity to model parameters are presented and possible consequences due to nocturnal nitrogen processing downwind of Fairbanks are discussed. This work has been prepared for submission to the journal *Atmospheric Chemistry and Physics*. As an exploratory study, Appendix A presents an experiment where the scenario used in MISTRA is adapted to Barrow, Alaska to explore production of $ClNO_2$ by reactions with N_2O_5 in an Arctic environment. Results from Chapter 2 and the appendix may serve as motivation for funding of future research efforts. Conclusions and outlook are summarized in Chapter 3.

1.10 References

Alaska Climate Research Center ACRC, 2010. "Alaska Climatology." <http://climate.gi.alaska.edu/Climate/index.html>

Alaska Department of Environmental Conservation (ADEC, 2008). Fairbanks non-attainment area boundary comments. Emissions inventory 2005. <http://www.dec.state.ak.us/air/doc/DEC_EPA_Fbks_NA_20oct08.pdf> Oct 2008. Last accessed: 22 Oct 2011.

Apodaca, R., Huff, D. and Simpson, W.: The role of ice in N_2O_5 heterogeneous hydrolysis at high latitudes, Atmos. Chem. Phys, 8, 7451–7463, 2008.

Ayers, J. D. and Simpson, W. R.: Measurements of N_2O_5 near Fairbanks, Alaska, J. Geophys. Res, 111(D14), D14309, doi:10.1029/2006JD007070, 2006.

Ayers, J., Apodaca, R., Simpson, W. and Baer, D.: Off-axis cavity ringdown spectroscopy: application to atmospheric nitrate radical detection, Applied optics, 44(33), 7239–7242, 2005.

Bertram, T. and Thornton, J.: Toward a general parameterization of N_2O_5 reactivity on aqueous particles: the competing effects of particle liquid water, nitrate and chloride, Atmos. Chem. Phys, 9, 8351–8363, 2009.

Brown, S., Ryerson, T., Wollny, A., Brock, C., Peltier, R., Sullivan, A., Weber, R., Dubé, W., Trainer, M., Meagher, J., Fehsenfeld, F., et al.: Variability in nocturnal nitrogen oxide processing and its role in regional air quality, Science, 331, 2006.

Brown, S., Dubé, W., Osthoff, H., Wolfe, D., Angevine, W. and Ravishankara, A.: High resolution vertical distributions of NO_3 and N_2O_5 through the nocturnal boundary layer, Atmos. Chem. Phys. Disc., 6(5), 9431–9458, 2007a.

Brown, S., Dubé, W., Osthoff, H. and Stutz, J.: Vertical profiles in NO_3 and N_2O_5 measured from an aircraft: Results from the NOAA P-3 and surface platforms during the New England Air Quality Study 2004, J Geophys. Res, 2007b.

Bytnerowicz, A., Percy, K., Riechers, G. and Padgett, P.: Nitric acid vapor effects on forest trees — deposition and cuticular changes, Chemosphere, 1998.

Dentener, F. J. and Crutzen, P. J.: Reaction of N_2O_5 on Tropospheric Aerosols: Impact on the Global Distributions of NO_x, O_3, and OH, J. Geophys. Res, 98, 7149-7163, 1993.

Driscoll, C. T., Lawrence, G. B., Bulger, A. J., Butler, T. J., Cronan, C. S., Eagar, C., Lambert, K. F., Likens, G. E., Stoddard, J. L. and Weathers, K. C.: Acidic Deposition in the Northeastern United States: Sources and Inputs, Ecosystem Effects, and Management Strategies, BioScience, 51(3), 180, 2001.

Fairbanks North Star Borough (FNSB): Online maps. <http://www.co.fairbanks.ak.us/communityplanning/mapping.htm> Last accessed: 19 Nov 2011.

Fenn, M., Baron, J., Allen, E., Rueth, H., Nydick, K., Geiser, L., Bowman, W., Sickman, J., Meixner, T. and Johnson, D.: Ecological effects of nitrogen deposition in the western United States, BioScience, 53(4), 404–420, 2003.

Finlayson-Pitts, B. and Pitts, J.: Chemistry of the Upper and Lower Atmosphere, Academic Press, 2000.

Geyer, A. and Stutz, J.: Vertical profiles of NO_3, N_2O_5, O_3, and NO_x in the nocturnal boundary layer: 2. Model studies on the altitude dependence of composition and chemistry, J. Geophys. Res, 109(D12), D12307, 2004.

Graedel, T. E. and Keene, W. C.: Tropospheric budget of reactive chlorine, Global Biogeochem. Cycles, 9(1), 47, doi:10.1029/94GB03103, 1995.

Hanson, D.: Reaction of N_2O_5 with H_2O on bulk liquids and on particles and the effect of dissolved HNO_3, Geophys. Res. Lett., 24, 1087-1090, 1997.

Hanson, D. R. and Ravishankara, A. R.: The Reaction Probabilities of $ClONO_2$ and N_2O_5 on 40 to 75% Sulfuric Acid Solutions, J. Geophys. Res, 96(D9), 17307–17314, doi:10.1029/91JD01750, 1991.

Hauglustaine, D., Granier, C. and Brasseur, G.: The importance of atmospheric chemistry in the calculation of radiative forcing on the climate system, J. Geophys. Res, 99, 1173-1186, 1994.

Honrath, R., Lu, Y., Peterson, M., Dibb, J., Aresenault, M., Cullen, N. and Steffen, K.: Vertical fluxes of NOx, HONO, and HNO3 above the snowpack at Summit, Greenland, Atmospheric Environment, 36, 2629-2640, 2002.

Hough, A.: Development of a two-dimensional global tropospheric model: Model chemistry, J. Geophys. Res, 1991.

Hu, J. H. and Abbatt, J. P. D.: Reaction Probabilities for N 2O 5Hydrolysis on Sulfuric Acid and Ammonium Sulfate Aerosols at Room Temperature, The Journal of Physical Chemistry A, 101(5), 871–878, doi:10.1021/jp9627436, 1997.

Huff, D.: The role of ice surfaces in affecting nighttime removal of nitrogen oxides in high latitude plumes, PhD Thesis, University of Alaska Fairbanks, 1–154, 2010.

Huff, D. M., Joyce, P. L., Fochesatto, G. J. and Simpson, W. R.: Deposition of dinitrogen pentoxide, N_2O_5, to the snowpack at high latitudes, Atmos. Chem. and Phys., 11(10), 4929–4938, doi:10.5194/acp-11-4929-2011, 2011.

Jaffe, D. A. and Zukowski, M. D.: Nitrate deposition to the Alaskan snowpack, Atmospheric Environment, 27A, 2935-2941, 1993.

Jobson, B. T., Niki, H., Yokouchi, Y., Bottenheim, J., Hopper, F. and Leaitch, R.: Measurements of C 2-C 6hydrocarbons during the Polar Sunrise 1992 Experiment: Evidence for Cl atom and Br atom chemistry, J. Geophys. Res, 99(D12), 25355–25368, doi:10.1029/94JD01243, 1994.

Kanakidou, M., Singh, H., Valentin, K. and Crutzen, P.: A two-dimensional study of ethane and propane oxidation in the troposphere, J. Geophys. Res, 96, D8, 15395-15413, 1991.

McNeill, V., Patterson, J., Wolfe, G. and Thornton, J.: The effect of varying levels of surfactant on the reactive uptake of N 2 O 5 to aqueous aerosol, Atmospheric Chemistry and Physics Discussions, 6(1), 17–43, 2006.

Mentel, T. F., Sohn, M. and Wahner, A.: Nitrate effect in the heterogeneous hydrolysis of dinitrogen pentoxide on aqueous aerosols, Phys. Chem. Chem. Phys., 1(24), 5451–5457, doi:10.1039/a905338g, 1999.

Mozurkewich, M. and Calvert, J. G.: Reaction possibility of N_2O_5 on aqueous aerosols, J. Geophys. Res, 93, D12, 15889-15896, 1988.

Osthoff, H., Roberts, J., Ravishankara, A., Williams, E., Lerner, B., Sommariva, R., Bates, T., Coffman, D., Quinn, P., Dibb, J., Stark, H., et al.: High levels of nitryl chloride in the polluted subtropical marine boundary layer, Nature Geoscience, 1, 2008.

Seinfeld, J. H. and Pandis, S. N.: Atmospheric chemistry and physics: from air pollution to climate change, 2nd ed, 2006.

Sommariva, R., Osthoff, H., Brown, S., Bates, T., Baynard, T., Coffman, D., de Gouw, J., Goldan, P., Kuster, W. and Lerner, B.: Radicals in the marine boundary layer during NEAQS 2004: a model study of day-time and night-time sources and sinks, Atmos. Chem. Phys. Disc., 8(4), 16643–16692, 2008.

Stevens, C. J., Dise, N. B., Mountford, J. O. and Gowling, D. J.: Impact of Nitrogen Deposition on the Species Richness of Grasslands, Science, 303(5665), 1876–1879, doi:10.1126/science.1094678, 2004.

Stutz, J., Alicke, B., Ackermann, R. and Geyer, A.: Vertical profiles of NO_3, N_2O_5, O_3, and NO_3 in the nocturnal boundary layer: 1. Observations during the Texas Air Quality Study 2000, J Geophys. Res, 109, D12306, 2004.

Thornton, J. A., Kercher, J. P., Riedel, T. P., Wagner, N. L., Cozic, J., Holloway, J. S., Dubé, W. P., Wolfe, G. M., Quinn, P. K., Middlebrook, A. M., Alexander, B., et al.: A large atomic chlorine source inferred from mid-continental reactive nitrogen chemistry, Nature, 464(7286), 271–274, doi:10.1038/nature08905, 2010.

Van Doren, J., Watson, L., Davidovits, P., Worsnop, D., Zahniser, M. and Kolb, C.: Uptake of N_2O_5 and HNO_3 by aqueous sulfuric acid droplets, J. Phys. Chem., 95, 1684-1689, 1991.

von Glasow, R., Sander, R., Bott, A. and Crutzen, P.: Modeling halogen chemistry in the marine boundary layer. 1. Cloud-free MBL, J. Geophys. Res, 107(43418211), 4352, 2002.

Wesely, M.: Parameterization of surface resistances to gaseous dry deposition in regional-scale numerical models, Atmospheric Environment (1967), 23, 1293-1304, 1989.

Wesely, M. and Hicks, B.: A review of the current status of knowledge on dry deposition, Atmospheric Environment, 34(12-14), 2261–2282, 2000.

Wood, E., Bertram, T. and Wooldridge, P.: Measurements of N_2O_5, NO_2, and O_3 east of the San Francisco Bay, Atmos. Chem. Phys., 5, 483-491, 2005.

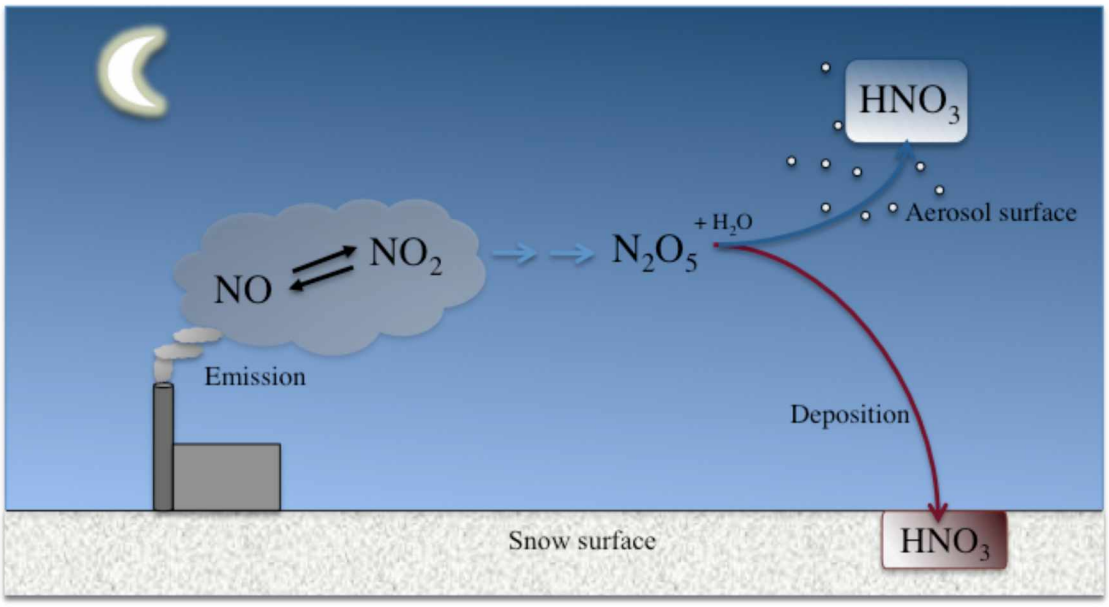

Fig. 1.1: NO_x removal from the gas phase can occur through reactions on aerosol surfaces or dry deposition.

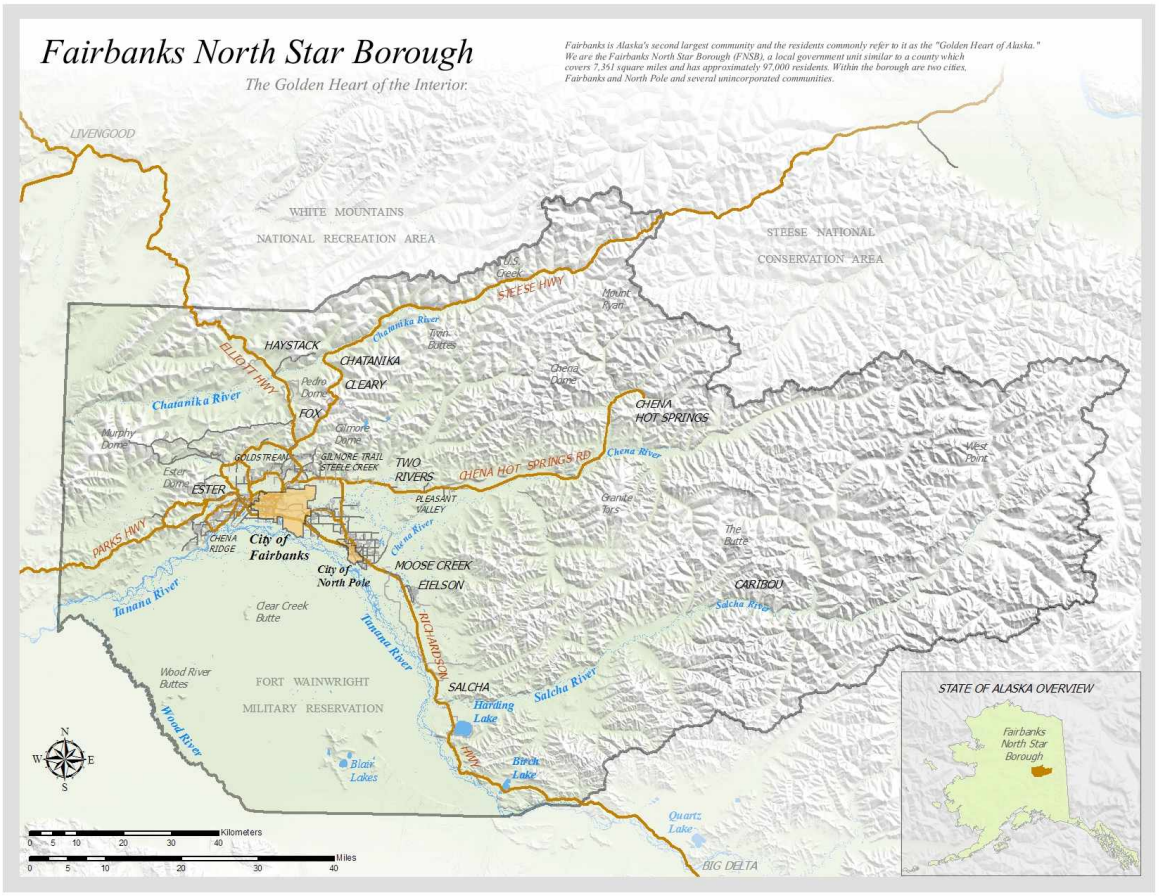

Fig. 1.2: Fairbanks North Star Borough area boundary. Figure courtesy of Fairbanks North Star Borough (FNSB, 2011).

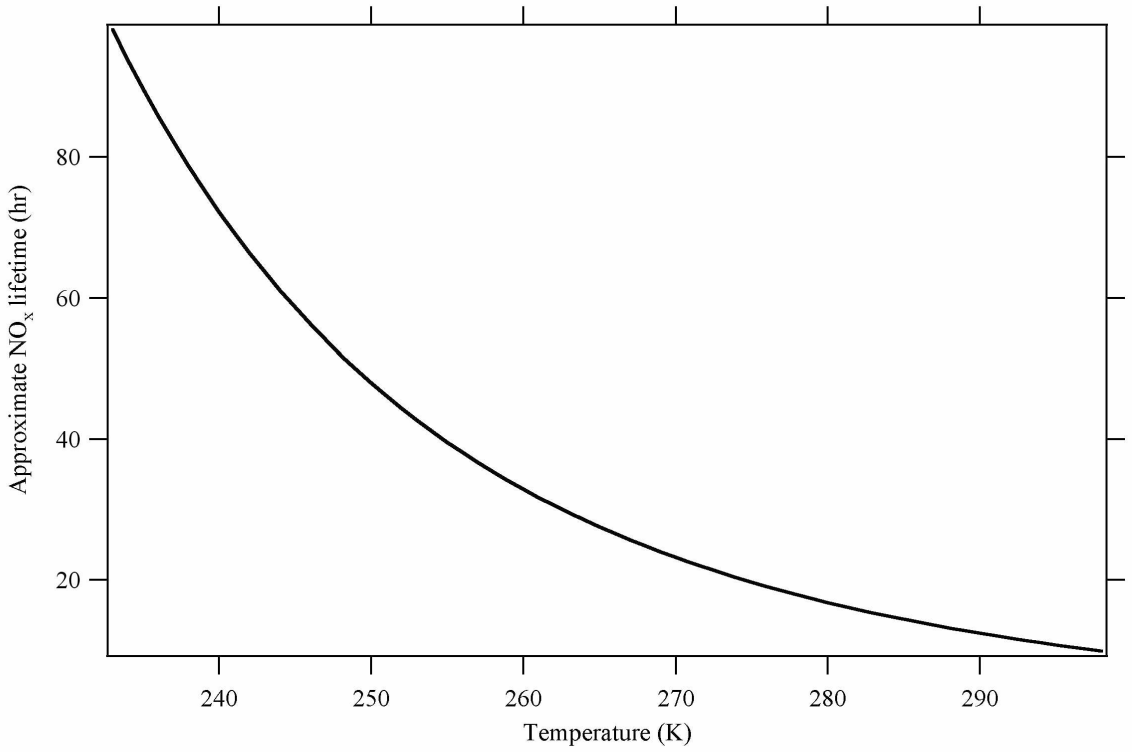

Fig. 1.3: Temperature dependence on lifetime of NO_x was estimated by calculations of the kinetic limitation of reaction (R2) in the nocturnal nitrogen oxidation pathway.

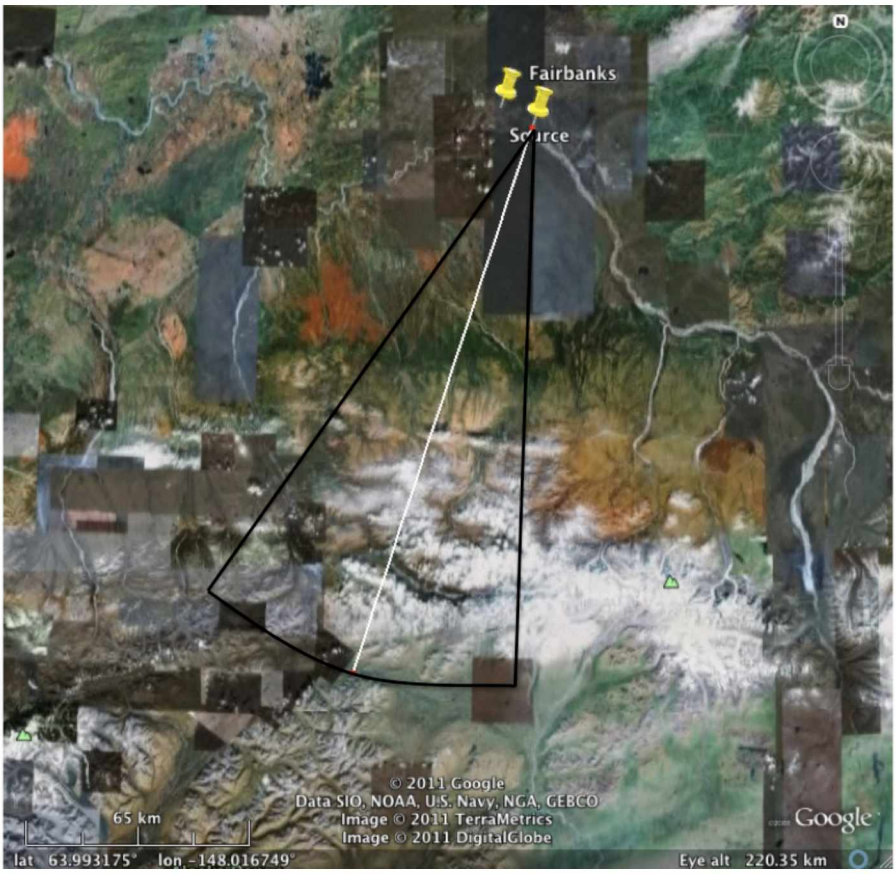

Fig. 1.4: Estimated area of deposition for experiment. Estimated area of downwind plume for initial deposition experiment as presented in Section 1.8 based on average wind speed and direction for November in Fairbanks and reaction rates at 258 K.

Table 1.1: Parameters for reactive uptake equation. Parameters used to describe γ in the parameterization presented by Bertram and Thornton (2009) and shown in equation (1.3). For simplicity and inclusion into the model to be discussed in the Chapter 3 the standard deviations from their study of these parameters have been removed.

Parameter	Value
A (s)	3.2×10^{-8}
β (s^{-1})	1.15×10^{6}
δ (M^{-1})	1.3×10^{-1}
ϕ	6.0×10^{-2}
ξ	29

Chapter 2: The fate of NO_x emissions due to nocturnal oxidation at high latitudes: 1-D simulations and sensitivity experiments[1]

The fate of nitrogen oxide pollution during high-latitude winter is controlled by reactions of dinitrogen pentoxide (N_2O_5) and is highly affected by the competition between heterogeneous atmospheric reactions and deposition to the snowpack. MISTRA, a 1-D photochemical model, simulated an urban pollution plume from Fairbanks to investigate this competition of N_2O_5 reactions and explore sensitivity to model parameters. It was found that dry deposition of N_2O_5 made up a significant fraction of N_2O_5 loss near the snowpack, but reactions on aerosol particles dominated loss of N_2O_5 over the integrated atmospheric column. Sensitivity experiments found the fate of NO_x emissions were most sensitive to NO emission flux, photolysis rates, and ambient temperature. The results indicate a strong sensitivity to urban area density (affecting NO flux), season and clouds (affecting photolysis), and climate (affecting temperature), implying a strong sensitivity of the results to urban planning and climate change. Results suggest that secondary formation of $PM_{2.5}$ nitrate in the Fairbanks downtown area does not contribute significant mass to the total $PM_{2.5}$ concentration, but appreciable amounts are formed downwind of downtown due to nocturnal NO_x oxidation and subsequent reaction with ammonia on aerosol particles.

---

[1] Joyce, P.J., von Glasow, R., and Simpson, W.R.: The fate of NO_x emissions due to nocturnal oxidation at high latitudes: 1-D simulations and sensitivity experiments, Atmospheric Chemistry and Physics, in preparation for submission December 2011.

2.1 Introduction

The high-latitude winter is a unique chemical environment characterized by extreme cold, extended periods of darkness, and constant snow cover. As the world's population increases, high latitudes are likely to see increased population, enhanced urbanization, and increased resource extraction, all leading to increased pollution emissions including nitrogen-containing species. Anthropogenic nitric oxide (NO) and nitrogen dioxide (NO_2) emissions form the chemical family of NO_x, which are ultimately removed from the atmosphere through oxidation to form nitric acid (HNO_3). Nitric acid can acidify aerosol particles in the atmosphere or deposit to the ground where it has been found to adversely affect ecosystems (Fenn et al., 2003). In sunlit conditions, the principal removal pathway of NO_2 is reaction with OH (Seinfeld and Pandis, 2006) and this reaction can form significant amounts of HNO_3 during the day, particularly in polluted regions (Finlayson-Pitts and Pitts, 2000). In the absence of photolysis, the "dark" reaction pathway forms the intermediate species nitrate radical (NO_3) and dinitrogen pentoxide (N_2O_5), which have both been measured in the nocturnal boundary layer (Brown et al., 2003; Ayers and Simpson, 2006; Sommariva et al., 2008). The dark reaction pathway includes reactions (R1) to (R3), followed by either reaction (R4a) or (R4b):

$$NO + O_3 \longrightarrow NO_2 + O_2 \quad \text{(R1)}$$

$$NO_2 + O_3 \longrightarrow NO_3 + O_2 \quad \text{(R2)}$$

$$NO_2 + NO_3 + M \underset{\leftarrow}{\longrightarrow} N_2O_5 + M \quad \text{(R3)}$$

$$N_2O_5 + H_2O \xrightarrow{surface} 2HNO_3 \quad \text{(R4a)}$$

$$N_2O_5 + Cl^- \xrightarrow{surface} ClNO_2 + NO_3^- \quad \text{(R4b)}$$

The absence of photolysis allows NO_3 to exist in sufficient concentration for reaction (R3) to occur and cold temperatures hinder the dissociation of N_2O_5, making the cold and dark conditions of high-latitude winter ideal for N_2O_5 formation. Upon formation, N_2O_5 can undergo heterogeneous hydrolysis through reaction (R4a) on the surface of an aerosol particle in the atmosphere or the snowpack surface on the ground to form HNO_3. Figure 2.1 outlines the dark oxidation pathway reaction sequence and the competing removal of N_2O_5 by reactions on aerosol particles and the snowpack through reaction (R4a). Alternatively, N_2O_5 can react through reaction (R4b) with Cl^- after uptake in an aerosol particle to form nitryl chloride ($ClNO_2$), which is volatile and quickly enters the gas phase.

Cold and dark conditions of high-latitude winter encourage loss of NO_x via the dark oxidation pathway. In a modeling study, Dentener and Crutzen (1993) found that 80% of high latitude NO_x is lost through the dark oxidation pathway in winter. Measurements by Wood et al. (2005) at mid latitudes found total HNO_3 produced by N_2O_5 hydrolysis during the night can be comparable to ambient NO_2 concentrations,

suggesting total HNO_3 produced by heterogeneous hydrolysis may be greater at high latitudes during winter.

The probability of a heterogeneous reaction of N_2O_5 to occur upon a molecular collision with an aerosol particle surface is described through the reactive uptake coefficient, γ. Laboratory and field studies have shown γ can be affected by aerosol particle chemical composition (Hanson and Ravishankara, 1991; Van Doren et al., 1991). In a mid-latitude flight campaign, Brown et al. (2007b) observed a strong dependence of γ on particle acidity and composition. Laboratory analysis has found high concentrations of NO_3^- in aerosol particles can hinder uptake of N_2O_5 and suppress γ in a phenomena known as the "nitrate effect". Additionally, reaction (R4b) was presented by Graedel and Keene (1995) as a sink of N_2O_5 and has been observed in the atmosphere (Oshthoff et al, 2008; Thornton et al. 2010). Bertram and Thornton (2009) found trace amounts of Cl^-, when the molar $Cl^-/NO_3^- > 0.1$, can negate the nitrate effect. They have characterized γ's dependence on aerosol liquid water content, aqueous Cl^- concentration, and aqueous NO_3^- concentration in a parameterization for mixed organic and inorganic aerosol particles.

Since pollution is typically emitted at ground level, vertical gradients of reactive nitrogen species can easily form in nocturnal boundary layers, especially in cold and stable conditions. Observations of vertical distributions of NO_3 and N_2O_5 demonstrated that nocturnal mixing ratios can vary widely over vertical scales of 10 m or less, implying that NO_3 and N_2O_5 occupy distinctly different chemical regimes as a function of altitude (Brown et al., 2007a). Aircraft observations of NO_3 and N_2O_5 show that these species occur at larger concentrations and are longer lived aloft than they are near the ground

(Brown et al., 2007b). A modeling study by Geyer and Stutz (2004) found that slow upward transport of NO emitted near the ground, and the simultaneously occurring chemistry, controlled the vertical structure of the chemistry of NO_x, NO_3, and N_2O_5.

Such observations of vertical gradients of nocturnal nitrogen species may be due to competition between the removal of N_2O_5 through reaction (R4a) or (R4b) on aerosol particle surfaces aloft versus deposition to the snowpack at ground level. Measurements of N_2O_5 near Fairbanks in winter by our group found sinks of N_2O_5 (presumably heterogeneous chemistry) were an efficient mechanism for NO_x removal near ground level (Ayers and Simpson, 2006). Apodaca et al. (2008) found that dry aerosol surface area was insufficient to explain the loss of N_2O_5 observed, suggesting loss to other surfaces plays a key role. To characterize loss to the snowpack, Huff et al. (2011) found the deposition velocity of N_2O_5 to be 0.59 ± 0.47 cm s^{-1} and that dry deposition represents at least 1/8th of the total chemical removal of N_2O_5 near the ground. Understanding the magnitude of relative loss rates is essential for interpretation of N_2O_5 measurements performed at ground level since air parcels near the ground surface will undergo both loss to aerosol particles and the snowpack.

Here we use a 1-D atmospheric chemistry model to address the fate of emitted NO_x in high-latitude winter. A 1-D model allows for analysis of a theoretical atmospheric column composition versus height over time and comparison of loss processes, such as reaction of N_2O_5 on aerosol particles versus the snowpack. Timescales for removal of NO_x are analyzed and model sensitivities to parameters and constraints are examined.

2.2 Model description

2.2.1 General features

The meteorological and microphysical part of MISTRA (MIcrophysical STRAtus) was originally a cloud-topped boundary layer model used for microphysical simulations of stratus clouds (Bott and Trautmann, 1996). MISTRA has been adapted as a marine boundary layer model for studies of polar halogen chemistry (von Glasow et al., 2002; Piot and von Glasow, 2008; von Glasow et al., 2008) and includes gas phase, liquid phase, and heterogeneous chemistry, as well a microphysical module that explicitly calculates particle growth and treats interactions between radiation and particles. Aerosol particles are initialized as the sum of three lognormal modes based on Jaenicke (1993) and distributed into 70 bins by diameter. Calculations of kinetic rates are governed by IUPAC (International Union of Pure and Applied Chemistry) rate constants. Mixing is driven by turbulent heat exchange coefficient calculations. The model has 150 vertical layers with a 10 m vertical resolution from the bottom layer centered at a height of 5 m. The model runs have a 10 s integration time with output every 15 minutes. For a more detailed explanation of the model see von Glasow et al. (2002).

MISTRA was modified to treat dry deposition of gases to the snowpack as an irreversible removal from the lowest atmospheric layer (5m) to the snowpack below using a resistance model presented by Wesely (Wesely, 1989; Seinfeld and Pandis, 2006). The parameterization includes aerodynamic, quasi-laminar, and surface resistance and utilizes gas to aqueous equilibrium coefficients explicitly calculated for each species by MISTRA. Parameters for a mixed forest with wetland in a winter, sub-freezing

environment were chosen (Wesely, 1989) and include resistance to deposition by buoyant convection and a lower ground "canopy" to simulate resistance to uptake by leaves, twigs, and other exposed surfaces. No resistance to deposition by large vegetation resistance is simulated. Dry deposition of NO has been found to be negligible by Wesely and Hicks (2000) and is calculated properly by the resistance model in MISTRA. A dry deposition velocity of 0.59 cm s^{-1} is explicitly specified for N_2O_5, based on the field study by Huff et al. (2011), while all other dry deposition velocities are calculated using the parameterization by Wesely (1989). Significant dry deposition in the model occurs for species of interest NO_2, O_3, N_2O_5, and HNO_3.

The parameterization presented by Bertram and Thornton (2009) is included to calculate $\gamma_{N_2O_5}$ explicitly for each model layer in time. By this parameterization, $\gamma_{N_2O_5}$ is dependent on aqueous NO_3^- concentration, aqueous Cl^- concentration, and aerosol particle liquid water content.

To simulate a high-latitude atmospheric column moving in space, MISTRA is initialized as a clean Arctic air mass that then receives a pollution injection for two hours, corresponding to the contact time of an air parcel moving over Fairbanks at a speed of about 1 m s^{-1}. Model runs begin at local midnight (t=0 h), with pollution injection period beginning at t=2 h and ending at t=4 h. Injection occurs as a positive flux from the ground surface into the lowest model layer (5 m). No additional injection occurs after t=4 h and simulations continue until t=50 h for analysis two days "downwind" of the pollution source to focus on the fate of emitted NO_x.

2.2.2 Observational constraints

Model runs did not attempt to simulate a single day for comparison with observations, but rather are presented to study the detailed chemical processes occurring under idealized conditions. The "base case" scenario is initialized as an average November day with a clear sky and snow covered ground with an albedo of 0.8. Photolysis rate calculations are performed for November 10 at latitude 64.76°N, with a sunrise of 8:03 and a sunset of 15:57. Both daytime and nighttime chemistry occur in the model. Photolysis rate calculations use a total column ozone of 401 Dobson Units based the average of November 2009 observations over Fairbanks from the Total Ozone Mapping Spectrometer (TOMS, 2011). An initial temperature at ground level of 257K (Fig. 2.2) is an observational average from 1929-2010 for November (ACRC, 2011). Relative humidity (RH) is constrained to 78% in the mixed layer for the base case (Fig. 2.2) based on average of November 2009 observations from the meteorological station located at the Fairbanks International Airport courtesy of the National Climate Data Center (NCDC, 2011).

Vertical mixing at high latitudes can become extremely hindered due to temperature inversions caused by strong radiative cooling from the ground surface at night. A nocturnal in-situ vertical profile of NO_2 obtained from the Arctic Research of the Composition of the Troposphere from Aircraft and Satellites (ARCTAS) campaign is used to constrain chemical vertical profiles in such conditions (ARCTAS, 2008). The flight originated at Fairbanks International Airport and took off at 02:23 AKST on April 8, 2008. NO_2 was detected to an altitude of 300 m along a flight path to the southwest,

away from and downwind of downtown Fairbanks. The temperature profile obtained from the April 8, 2008 flight showed a surface inversion to 50 m and a capping inversion at 300 m. Vertical mixing in stable conditions presents problems in model simulations. Attempts to simulate chemical profiles based on temperature profile observations did not yield results that agreed with the chemical profiles. Therefore, a mixed layer of 300 m is initialized using a dry-adiabatic lapse rate from the ground capped by a small isothermal layer (Fig. 2.2). The modeled vertical temperature profile allows for mixing of NO_2 throughout the mixed layer to agree with the observed chemical vertical profile.

The chemical composition of the modeled atmospheric column at t=0 h represents an unpolluted Arctic air mass. Ambient ozone mixing ratios from Barrow, Alaska are 35 ppb_v on average from 2000-2010 in November, with peak abundances of 42 pbb_v (ESRL, 2011) and concentrations of polar aerosols found close to surface are generally very low (Seinfeld and Pandis, 2006). Therefore, the background chemical composition of the model is initialized as devoid of anthropogenic pollutants with an O_3 mixing ratio of 40 ppb_v and an aerosol loading of <1 $\mu g\ m^{-3}$.

The pollution injection during the "emission period" consists of NO, sulfur dioxide (SO_2), ammonia (NH_3), and aerosol particles containing organic matter and sulfuric acid (H_2SO_4) (Table 1). Sufficient NO_x concentrations can "titrate" an air mass through reactions (R1) and (R2), depleting O_3 and leading to an environment with excess NO, which is observed almost nightly in winter months in downtown Fairbanks (State of Alaska, 2008). The modeled NO flux is the smallest emission rate possible to titrate ozone to near zero through reactions (R1) and (R2). This yields a modeled NO_x mixing

ratio at the end of the pollution injection period (t=4 h) within the first quartile (Q1) to third quartile (Q3) range of 31-103 ppb_v from observations in downtown Fairbanks (State of Alaska, 2008) and simultaneously brings O_3 down to 1 ppb_v at ground level. Emission of SO_2 is constrained by Nov. 2008 average abundance observed in downtown Fairbanks (State of Alaska, 2008).

Ammonia and aerosol particle emissions are interrelated. Modeled aerosol particles are emitted as liquid droplets containing organic material, sulfuric acid (H_2SO_4), and trace amounts of chloride and are constrained by $PM_{2.5}$ (aerosol particles with aerodynamic diameter <2.5μm) observations from downtown Fairbanks (ADEC, 2007) (Table 1). To obtain an appropriate aerosol number density and surface area, the number density of a standard tri-modal urban aerosol distribution (Jaenicke, 1993) is scaled to agree with the average $PM_{2.5}$ mass observation for November (ADEC, 2007). Sulfate (SO_4^{2-}) concentrations from emitted H_2SO_4 are constrained on a percent mass basis based on total $PM_{2.5}$. Remaining observed aerosol particulate mass composed primarily of organic carbon, elemental carbon, and heavy metals is accounted for in the model using chemically inert dissolved organic matter.

Currently, there are no known ammonia observations in Fairbanks. Ammonia mixing ratios in remote areas can be <50 ppt_v (Finlayson-Pitts and Pitts, 2000), so background NH_3 was initialized as 0.05 ppb_v. Upon contact with aerosol particles, NH_3 readily protonates in acidic particles to form ammonium (NH_4^+), increasing the pH. The molar ratio of NH_4^+/SO_4^{2-} in aerosol particles can be used to determine aerosol acidity, where a value above 2 indicates that all sulfuric acid has been neutralized. Data from

downtown Fairbanks shows the Q1 – Q3 range of molar NH_4^+/SO_4^{2-} to be 1.5 - 2.4 (State of Alaska, 2011). Modeled NH_3 emission from the ground is constrained to be 4.8% of the NO_x emission (discussed in Sect. 5.2), and is 3x the molar H_2SO_4 emission. This leads to values of NH_4^+/SO_4^{2-} = 1.5 at the end of the pollution injection period through aerosol particle uptake (Table 1).

2.3 Results

2.3.1 Urban pollution plume

The evolution of modeled primary emissions, destruction of ozone, and resulting oxidation products are shown in Figs. 2.3 & 2.4. All pollutants rapidly mix upon emission to 100 m at t=4 h, reaching 300 m at approximately t=8 h, then slowly dilute higher for the duration of the model run. The NO_x vertical profile (Fig. 2.3a) shows a strong negative gradient with increasing height at the end of the emission period due to ground level emission. Emitted NO_x reaches 100 m at the end of the emission period and 300 m, the top of the initialized mixed layer, within 2 hours.

Modeled total $PM_{2.5}$ (Fig. 2.3b) shows a vertical profile similar to NO_x in the first two hours after the emission period ends (t=6 h) due to vertical dilution. No observations of aerosol number density and surface area are available for downtown Fairbanks for validation. Modeled values at ground level at t=4 h reach a number density of $2x10^4$ cm^{-3} and aerosol surface area of 380 μm^2 cm^{-3}. Modeled nitrate produced through secondary formation by reaction (R4a) and (R4b) in aerosol particles is 2% of total $PM_{2.5}$ mass at

t=4 h, compared to an average observed value of 4.4% total $PM_{2.5}$ mass in November (ADEC, 2007).

Background and emitted ammonia rapidly react with emitted acidic aerosol particles, forming particulate ammonium (Fig. 4f). Modeled ammonium in aerosol particles is 5% by mass at t=4 h, and closely resembles ammonium observations comprising 6.4% of total $PM_{2.5}$ mass (State of Alaska, 2011). Particulate ammonium formation after the emission period increases the molar ratio of NH_4^+/SO_4^{2-} to 2.1 at t=5 h. Column integrated SO_2 remains constant in time, indicating that the model does not produce significant amounts of sulfate in the base case, and the only loss mechanism of SO_2 from the atmosphere is dry deposition (not shown).

2.3.2 Plume evolution in base case

Previous field studies in Fairbanks were performed outside of the downtown area in order to observe un-titrated air masses that allow for formation of N_2O_5. Ayers and Simpson (2006) conducted measurements on the edge of the populated area of Fairbanks and observed both titrated and un-titrated air masses. Modeled dilution of NO_x (Fig. 2.3a) agrees well with various field measurements in the greater Fairbanks area (Table 2), where abundances of NO_x reduce with distance from downtown.

Background ozone (Fig. 2.4a) is depleted (<2 ppb_v) at ground level at t=4 h and is significantly reduced in the mixed layer due to titration of the air mass through reactions (R1) and (R2). Ozone abundance returns to near background approximately four hours

after the pollution injection due to vertical mixing and reformation of NO in daylight hours.

Abundance of N_2O_5 in the model (Fig. 2.4b) peaks aloft in the early morning of the first day (t=9 h) and in the middle of the second night (beginning t=21 h). The diurnal cycle of N_2O_5 shows it is not produced during daylight hours but can reform over one day after NO_x emission from the remaining NO_x in the atmosphere. A reduction in mixing ratio of N_2O_5 near the ground occurs due to dry deposition to the snowpack, which is an additional loss that only occurs from the lowest atmospheric layer.

Formation of $ClNO_2$ (Fig. 2.4c) occurs immediately upon formation of N_2O_5 through reaction (R4b) and removes trace Cl^- in emitted aerosol particles (not shown) in less than one hour after emissions end (t=6 h). A reduction in N_2O_5 mixing ratio below 50 m can be seen (Fig. 2.4b) from t=4 h to t=5 h due to $ClNO_2$ formation. Once formed, $ClNO_2$ dilutes through the mixed layer and abundances of ~20 ppt_v throughout the mixed layer are lost through photolysis during the first day resulting in peak concentrations of $2.6x10^3$ Cl radicals cm^{-3}. Formation of $ClNO_2$ is limited by aqueous Cl^- concentrations in this simulation.

Particulate nitrate (Fig. 2.4d) is primarily formed through reaction (R4a) and peaks ~24 hours after the emission period at the end of the second night, corresponding to loss of N_2O_5 formed during the second night. Formation of nitrate occurs through the dark oxidation pathway during the first day due to loss of pre-existing N_2O_5. Total nitrate (all aerosol particle sizes) peaks at a concentration of 6.0 μg m^{-3} at an altitude of 325 m at t=30 h, where 4.2 μg m^{-3} of the nitrate is in the $PM_{2.5}$ size fraction. Concentrations of

nitrate at ground level reach a maximum of 2.2 μg m^{-3} 16 hours after emission ends, showing a delay in secondary formation of nitrate through the dark oxidation pathway.

Gas phase nitric acid (Fig. 2.4e) mixing ratio peaks within hours after the nitrate aerosol peaks and is outgassed by particles made acidic through reaction (R4a). Larger aerosol particles are able to uptake greater amounts of NO_3^-. The peak number density of large aerosol particles (d > 2.5μm) occurs aloft, leading to increased NO_3^- aloft (Fig. 2.4d) and decreased abundance of gas-phase HNO_3 aloft (Fig. 2.4e). Under such weak photolysis conditions, HNO_3 does not react readily with other species and will be ultimately removed through aerosol uptake upon mixing or deposition to the snowpack.

Formation of NH_4^+ (Fig. 2.4f) occurs during the emission period and one hour immediately following emission due to aerosol particle uptake of NH_3 and neutralization of emitted sulfuric acid aerosol particles. This process depletes background ammonia and emitted ammonia throughout the column (not shown) and forms ammonium sulfate $[(NH_4)_2SO_4]$ or ammonium nitrate (NH_4NO_3) in the particles. Once ammonium in formed in the aerosol particles they are well-mixed throughout the mixed layer and no losses from the atmosphere exist except aerosol particle deposition to the snowpack. Some additional ammonium is produced after the emission period due to entrainment from background ammonia above the mixed layer.

2.3.3 Fate of NO_x in base case

Nitrogen speciation is divided into four categories (Fig. 2.1) to characterize the state of emitted NO_x in time. "Un-reacted" fraction includes NO_x, N_2O_5, and other

reactive nitrogen species present in sub-ppt_v (part-per-trillion): HONO, HNO_4, and N_2O_4. "Aerosol reacted" fraction includes any aqueous phase NO_3^-, HNO_3 outgassed from acidic particles, and $ClNO_2$ that remains suspended in the atmosphere. "N_2O_5 dry deposited" fraction represents heterogeneous hydrolysis on the snowpack at ground level and is dry deposition of N_2O_5 only. "Other deposited" fraction includes dry deposition of NO_2 and HNO_3 and wet deposition of NO_3^- aerosol. Reduced species NH_3 and NH_4^+ are not oxidized under simulation conditions and are not included in the speciation analysis.

Presented in Fig. 2.5 is a time series of speciation of emitted NO_x, depicted as the column integrated fraction of each species out of the total emitted NO_x. Diurnal cycles discernible include the formation of NO and destruction of N_2O_5 during the day. A vertical transect at any point in time depicts the current state of emitted NO_x. Most apparent is the trend of the un-reacted fraction decreasing in time. In the base case, only 36% of un-reacted nitrogen remains in the atmosphere two days after the beginning of emissions (t=50 h), with the remaining 63% partitioned among the other categories (Fig. 2.5). The large fraction of gas phase HNO_3 (33% at t=50 h) is due to acidic aerosol conditions and represents a significant fate of emitted NO_x. Night-time formation of HNO_3 dominates gas phase HNO_3 production, but a small amount of HNO_3 production can be seen in the afternoon periods due to the daytime oxidation pathway. Dry deposition of HNO_3 through the aerosol reacted pathway is the fate of 5% of the total emitted NO after two days, but is less than the N_2O_5 dry deposited fraction of 17%. Dry deposition of N_2O_5 makes up a discernable fraction two hours after the emission period ends while NO_3^- aerosol deposition and HNO_3 dry deposition does not build until 16

hours after the emission period ends. A slight increase in dry deposition occurs during the day due to increased turbulent mixing. Other reactive nitrogen species such as HONO, HNO_4, and N_2O_4 are included with the NO_2 fraction and make up an insignificant portion (< 1%).

2.4 Sensitivity of the fate of NO_x to model parameters

Experiments were performed to analyze the sensitivity of the fate of NO_x to model constraints by modifying parameters over ranges based on realistic conditions. These experiments are presented as demonstrations of model performance as well as representations of the base case under changing scenarios. Sensitivities found to be most significant are described below and are depicted in Fig. 2.6 (a-h). Analysis of each experiment is conducted by relative comparison of total nitrogen fractions two days after the emission period ends (t=50 h).

a) NO emission rate: Increased flux of NO during the emission period leads to increased NO_x abundance, most intensely near the ground. Increased mixing ratio of NO depletes O_3 in the mixed layer, slowing reactions (R1) and (R2) and N_2O_5 formation. This slowing of N_2O_5 formation causes the un-reacted fraction to remain dominant. The 5x-NO case represents a strongly titrated air mass. In this case, modeled NO_x reaches 300 ppb_v at t=4 h, within the range of downtown observations (Table 1), leaving excess NO and depleted ozone at night throughout the mixed layer for the entire duration of the run, suppressing N_2O_5 formation and slowing nocturnal

oxidation of NO_x. Alternatively, under a lower NO emission rate, NO_x is efficiently removed through the dark oxidation pathway, with preference for the aerosol reacted fraction.

b) NH_3 emission rate: Increased emissions of NH_3 lead to greater amounts of NO_3^- retention in the particulate phase, giving increased particulate surface area and thus a greater aerosol reacted fraction. This result was somewhat surprising because we expected that the increased nitrate effect from enhanced NO_3^- retention would decrease the reactive uptake coefficient and reduce the aerosol particle reactivity. However, the aerosol particle reactivity is the product of gamma and the aerosol surface area, and the surface area term increase outweighs the reduction of gamma in the simulation. This is discussed in further detail in Section 2.5.

c) Aerosol emission rate: In general, increased aerosol flux from the surface leads to greater aerosol particle number density, surface area, and mass density of sulfate particles. Primary sulfate emissions do not leave the particles and thus lead to increased total aerosol particle mass. The increase in aerosol particle surface area allows for more surface reactivity and increases the aerosol reacted fraction and aerosol particle deposition in the other deposited fraction over the 1/5x – 5x factor sensitivity experiments. Additionally, the N_2O_5 dry deposited fraction is decreased due to the enhanced aerosol uptake. The decrease of the aerosol reacted fraction in the 2x experiment requires further examination, but is likely a feedback based on NO_x emission and time of analysis (t=50 h).

d) N_2O_5 dry deposition velocity: The empirical value of dry deposition velocity of N_2O_5 was found to be between 0.12 – 1.06 cm s^{-1} and covered by the range of the 1/5x – 2x sensitivity experiments. Total fraction of N_2O_5 dry deposited varies from 5% to 25% over this range. Increases in the dry deposition velocity of N_2O_5 lead to an increase in the N_2O_5 dry deposited fraction, a corresponding decrease in all other fractions, and a reduction of N_2O_5 mixing ratio at ground level, near the snowpack.

e) Photolysis: In this experiment, photolysis calculations are carried out for 10 November, 21 December, 22 January, 21 February, and 20 March. The lowest photolysis rate (21-Dec) corresponds to the smallest un-reacted fraction. Under the weakest photolysis conditions, N_2O_5 is present at all hours and reaches a minimum value of 200 ppt_v throughout the mixed layer during the day. This allows for nitrate formation via the dark oxidation pathway through reaction (R3) for 24 hours per day. Increased photolysis and longer periods of daylight (20 March) leads to an increased un-reacted fraction due to limitation of reaction (R3) during the shorter nights and weak daytime oxidation of NO_x. Monthly average temperatures in winter in Fairbanks are very similar due to large temperature fluctuations over a monthly time period, and each month is likely have days near the base case temperature of 258 K. For a sensitivity experiment with respect to temperature, see (g).

f) Initial RH: This experiment modifies the initial RH in the mixed layer. Increases in RH lead to increases in aerosol surface area from water vapor to particle equilibrium calculated by the model. Most substantial in a relatively dry mixed layer, a 20% increase in RH from 40% to 60% increase the aerosol reacted fraction by 9%.

g) Surface temperature: For this experiment, temperature at bottom layer of the atmosphere ranges from 228 K to 273 K, which could occur on any given day during the months of November to March. Changes in surface temperature are reflected through the entire column due to the calculation of temperature gradient in the column using the lapse rate. Decreasing temperatures produce a significantly greater un-reacted fraction due kinetic limitation of reactions.

h) Initial mixing height: The mixed layer in the model gradually rises in time (Fig. 2.2) due to mixing from above. Due to the time needed to mix air throughout the 300 m mixed layer (~6 h), the height of the mixed layer is constant at 100 m at the end of the emission period for all runs (100 m – 400 m) and therefore does not affect constrained mixing ratios of emissions. Thus, this experiment shows variation of the dilution downwind of the emission source due to a variable mixed layer height. Increases in the height of the mixed layer decrease both N_2O_5 dry deposited and other deposited fractions while increasing the amount of aerosol reacted fraction retained in the atmosphere due to less contact with the snowpack surface.

i) Chloride concentration (not pictured): In this experiment, aqueous concentration of emitted chloride in aerosol particles varies from zero - 5x to determine effect on γ. The parameterization of γ and fate of NO_x is insensitive to Cl^- concentrations over this range, which leads to concentrations of 0.07 – 0.56 μg m^{-3} at t=4 h near the ground. Trace amounts of Cl^- present in the particles, however, reduce the aerosol reacted fraction, while the aerosol reacted fraction increases by 3% when no Cl^- is included. This result is likely due to analysis occurring two days after emission.

Analysis less than eight hours after emissions end would yield a larger sensitivity to Cl^- due to the presence of $ClNO_2$ in the aerosol reacted fraction. Significant reductions in N_2O_5 mixing ratio and nitrate production are seen (Fig. 2.4b) in the first hours after emission ends due to production of $ClNO_2$. Chloride concentrations may have a much greater impact on a local scale.

j) Time of day (not pictured): Variations of the time of day of emission period start is performed to analyze the effect of photolysis on the fresh or aged plume. With respect to local impacts (under 8 h), time of day has a significant effect on column composition by hindering or allowing the dark oxidation pathway to occur immediately after emission. By t=50 h, however, the plumes are exposed to relatively equal amounts of sunlight and there is no significant effect on the fate of NO_x.

k) SO_2 emission (not pictured): Weak photolysis conditions in the base case do not allow for secondary formation of sulfate by SO_2 conversion. Therefore, SO_2 is inert in these simulations and the fate of NO_x is found to be insensitive to SO_2 emissions.

l) Dry deposition velocity (not pictured): An additional experiment was performed to include the "upper canopy" of the mixed forest in the dry deposition parameterization to simulate deposition to trees. Addition of an upper canopy parameter in the dry deposition equation leads to increases of dry deposition velocity of 10% for HNO_3, 16% for NO_3, and an order of magnitude for NO_2. The explicitly set value for dry deposition velocity of N_2O_5 is scaled up by 10% for this experiment, based on the result for HNO_3. Including the upper canopy results in a

4% increase in the other deposited fraction, primarily due to increased NO_2 deposition, and a <1% increase in the N_2O_5 dry deposited fraction. In this 1-D model, addition of deposition to the upper canopy of trees has an insignificant effect on the fate of NO_x.

2.5 Discussion

2.5.1 Model results and implications

The simulations in this experiment presented for qualitative analysis of the fate of anthropogenic NO_x pollution in a high-latitude environment are not without a few liabilities. Cloud formation is avoided in the model primarily because microphysical and chemical feedbacks would hinder the main focus of this study. Observations by Sommariva et al. (2008) found that that N_2O_5 removal by fog droplets was dominant when fog was present. Cloud formation would likely lead to dominance of N_2O_5 uptake aloft in large cloud particles, leading to less gas-phase HNO_3 and more nitrate aloft which could undergo long-range transport. Cloud formation would also affect photolysis rates in model layers below the cloud. Clear skies dominate synoptic conditions in the greater Fairbanks area in the winter months, supporting that the base case simulation is not weakened by the absence of clouds.

The temperature profile of the column necessary to achieve the modeled mixed layer does not represent an in-situ profile. In development of the base case, attempts to replicate atmospheric soundings with strong inversion layers common in the months of December, January, and February produced extremely hindered mixing. No vertical

profiles of NO_x are available that correspond to such nocturnal temperature profiles. The NO_2 detected by the ARCTAS aircraft at 300 m was 14 km from downtown Fairbanks (ARCTAS, 2008). Assuming column motion of about 1 m s^{-1}, 14 km would correspond to the modeled NO_x profile at t=8 h, which shows vertical dilution to ~290 m. The modeled temperature profile of the base case is applicable for conditions with relatively high mixed layers and weak inversions, which are common in the "shoulder" months of October, November, March and April. Mixing by this temperature gradient method is suitable for this study; however, mixing forced by eddy-diffusivity has been performed to match observed vertical profiles (Geyer and Stutz, 2004) and may be more appropriate for thermally inverted and stratified boundary layer simulations. However, vertically resolved chemical observations are required to apply the Geyer and Stutz (2004) method.

Additionally, horizontal entrainment is not included in the model for mass conservation purposes. Transport between vertical model layers occurs and is ensured to be in mass balance, but no dilution occurs from horizontal mixing of background air into the parcel. By estimation, an air parcel moving at 1 m s^{-1} is 167 km from Fairbanks at corresponding model time of t=50 h. The urban area of Fairbanks is ~16 km wide, yielding a length to width ratio of approximately 10:1 after two days. Transport over such a large distance with limited dilution is unlikely; however, mixing with background ozone would lead to less limitation of reactions (R1) and (R2) and more efficient removal of NO_x.

Lastly, aerosol particles in the simulations were represented as purely aqueous constituents. With respect to frozen water, observations by LIDAR in Fairbanks indicate

presence of super-cooled and mixed phase aerosols in high latitude environments at temperatures as low as 240 K, suggesting aqueous phase aerosols are present in temperatures well below freezing temperature of water (Fochesatto et al., 2005). Freezing of particles would have complex and currently poorly understood effects on reactivity. However, freezing is likely to occur on the two-day timescale, implying that more study of the structure and reactivity of ice particles is needed.

Modeled vertical profiles of N_2O_5 have implications for interpreting field measurements. Modeled N_2O_5 mixing ratio at 105 m is over 2x greater than at the surface in the one hour immediately following emission and consistently 10-15% greater for the duration of the model run. This suggests that observations carried out near the snowpack may yield abundances of N_2O_5 significantly lower than those aloft. More importantly, positive vertical gradients of N_2O_5 show the importance of dry deposition as a loss mechanism of N_2O_5 near the snowpack and reaffirms the result found by Huff et al. (2011). Airborne measurements of N_2O_5 in Fairbanks during winter are necessary to fully understand the vertical and spatial distribution of the plume.

Results from the base case speciation analysis (Fig. 2.5) have implications for local and long-range deposition effects. Dry deposition of N_2O_5 begins immediately upon formation of N_2O_5 and dominates the nitrogen flux to the snowpack during the night. Snowpack deposition of aerosol nitrate and gas-phase HNO_3 does not occur in significant amounts until 16 hours after emissions have ended. This indicates dry deposition of N_2O_5 dominates nitrogen deposition to the snowpack on a local scale, while particulate nitrate deposition is minimal. Alternatively, particulate nitrate can remain suspended in the local

atmosphere, undergo long-range transport, be diluted in transit, and removed by a precipitation event.

Observations of both titrated and un-titrated air masses in studies such as Ayers and Simpson (2006) indicate a wide variability of the oxidation capacity of the mixed layer. Sensitivity experiments presented here have shown NO_x emissions in the absence of photolysis can single-handedly transform the lower atmosphere from an oxidizing environment rich in ozone to a reduced environment with no oxidation capacity. Some values of NO_x observed in downtown Fairbanks are even greater than the modeled 5x-NO_x experiment (Fig. 2.6a) in which ozone was titrated in the mixed layer for two days. In reality, horizontal mixing may reduce the timescale of titration as background ozone is mixed in, but ozone reduction may linger for well over 24 hours downwind. Ozone titration is likely to be enhanced under stable meteorological conditions.

The photolysis experiment (Fig. 2.6e) has implications for environments at higher latitudes than Fairbanks, which sits at 64.76° N. The month of December, with the weakest photolysis and longest periods of darkness, shows the smallest un-reacted fraction. Dry deposition of N_2O_5 and aerosol reacted fractions are enhanced by extended darkness. Locations north of the Arctic Circle (66.56° N) will have days in which no photolysis will occur and N_2O_5 formation is hindered, allowing the dark oxidation pathway of NO_x to carry out 24 hours per day. Under total darkness conditions, local deposition of N_2O_5 is likely to be enhanced.

The drastic dependence of the fate of NO_x on temperature (Fig. 2.6g) shows ambient temperatures are the most important naturally-occurring factor controlling the

chemistry of the nocturnal NO_x plume. Dry deposition rates of N_2O_5 remain fairly constant over the temperature range, suggesting that the heterogeneous chemistry occurring is more strongly dependent on temperature than N_2O_5 formation. The range of temperatures studied are not uncommon in Fairbanks for the months of November to March. For temperatures lower than 228 K and stable meteorological conditions, NO_x may be near the snowpack for extended periods of time, enhancing dry deposition.

2.5.2 Ammonium nitrate formation

Downtown Fairbanks lies in a US Environmental Protection Agency non-attainment area for $PM_{2.5}$ (ADEC, 2008). A common concern in reducing total $PM_{2.5}$ lies in a non-linearity present in aerosols containing ammonium, nitrate, and sulfate. When excess ammonia is available ($NH_4^+/SO_4^{2-} > 2$), reductions in sulfate may be replaced by nitrate, leading to an increase of ammonium nitrate in the aerosol (Seinfeld and Pandis, p 483). Modeled nitrate concentrations in the polluted area (t=4 h) are < 0.5 μg m^{-3} and agree with observations (ADEC, 2007), but concentrations of > 2 μg m^{-3} NO_3^- are modeled within six hours after emissions end. These observations suggest that secondary nitrate formation due to NO_x oxidation is not a major contributor to $PM_{2.5}$ non-attainment because titration of O_3 slows N_2O_5 formation and thus formation of NO_3^- and HNO_3. Enhanced secondary formation of nitrate, however, may have implications further downwind of the polluted area.

In the NH_3 emission rate sensitivity experiment (Fig. 2.6b), the aerosol reacted fraction increases with increased ammonia emission. This can be seen in total $PM_{2.5}$

concentrations near the ground (Fig. 2.7) beginning two hours after end of emission due to formation of NH_4NO_3. During the emission period, primary emissions of H_2SO_4 and organic matter dominate total mass and are similar for each experiment. During the emission period and for ~2h afterward, NH_4NO_3 concentrations are zero and $NH_4^+/SO_4^{2-} < 2$ in the particle and sulfuric acid is not fully neutralized. Base case emissions of NH_3 are sufficient to bring the molar ratio of NH_4^+/SO_4^{2-} at the surface to 1.5 at t=4 h, which gradually increases to 2.1 at t=5 h. Values of $NH_4^+/SO_4^{2-} > 2$ are possible as NO_3^- is formed and available to react with NH_4^+ to form ammonium nitrate (NH_4NO_3) (Seinfeld and Pandis, 2006, p 479). Increases in NH_3 flux bring the NH_4^+/SO_4^{2-} ratio at the end of the emission period (t=4 h) to 1.9 for the 5x NH_3 run. Divergence of total $PM_{2.5}$ mass at t=8 h (Fig. 2.7) between the sensitivity studies is controlled by NH_3 emission and subsequent formation of NH_4NO_3. In this manner, secondary formation of nitrate particles is controlled in magnitude by ammonia flux and limited in timescale by nocturnal NO_x oxidation. In all cases, secondary aerosol mass continues to form during the first day while N_2O_5 is still present from nighttime formation (Fig. 2.7).

The timescale limitation of NH_4^+ uptake by NH_4NO_3 formation makes it impossible to infer NH_3 abundances downtown based on NH_4^+ measurements. It is likely that ammonia exists in excess while magnitude of NH_4^+ uptake depends on particle composition. Due to the timescale of nitrate formation, a decrease in primary sulfate emissions should reduce total $PM_{2.5}$ and not be replaced by an increase in particulate nitrate in the downtown area. Due to the unknown NH_3 abundance, large concentrations of NH_4NO_3 are possible and could result in soil fertilization downwind of Fairbanks.

Ammonia emissions inventories in Fairbanks are likely underestimated. Studies have shown gas-powered automobiles to be sources of ammonia (Baum et al., 2000, Bishop et al., 2010). Additionally, three-way catalytic converters in modern gas-powered automobiles are a source of ammonia (Kean et al., 2000). Biomass burning is also a well documented source for ammonia emission, suggesting combustion of local fuel in wood-stoves could be a significant NH_3 source (Yokelson et al., 1996; Yokelson et al. 1997; Agaki et al., 2011). Additionally, Yokelson et al. (1996) have shown ammonia to be the primary form of nitrogen emission from a smoldering fire; many wood-stoves in the Fairbanks area are smoldered to burn slowly.

The EPA emissions inventory for Fairbanks listed 1325 tons $year^{-1}$ (TPY) of carbon monoxide (CO) and 0 TPY NH_3 from wood-stoves and fireplaces in 2005 (ADEC, 2008). Assuming all woodstove emissions are produced in 6 months out of the year, this yields an estimate of 221 tons $month^{-1}$ (TPM) of CO. Studies of smoldering wood smoke composition by Yokelson et al. (1997) estimate NH_3 emissions from burning wood to be 10.8% of the CO emission for white spruce harvested in Alaska. Assuming local fuel is consumed in woodstoves, the estimation using Yokelson et al. (1997) would yield 24 TPM NH_3, currently un-accounted for in the emissions inventory. For mobile sources, the emissions inventory reports 71 TPM NO_x and 4 TPM NH_3 from annually occurring on-road, gas-powered sources. Calculations based on results from a study by Kean et al. (2000) suggest the magnitude of NH_3 emissions are 25% that of NO_x from automobiles due to use of 3-way catalyst systems in gas-powered vehicles. By this estimate, on-road NH_3 from gas-power vehicles is 18 TPM, an estimate 4.5x higher than

the value listed in the inventory. Together, these estimates for NH_3 emissions from woodstoves and automotive sources make for 42 TPM NH_3, which is 4.8% of the total reported NO_x emission of 872 TPM. Ammonia flux in the base case was constrained by this percentage of NO_x emissions and yielded a value of 0.96 μg m^{-3} NH_4^+ and 1.6 ppb_v excess NH_3 near the ground at the end of the emission period (t=4 h). In order to achieve the measured November average of 0.97 μg m^{-3} NH_4^+ (State of Alaska, 2011) through aerosol uptake, we estimate a total of 1.2 ppb_v NH_3 need be available for uptake into aerosol particles. The base case emitted NH_3 was sufficient to reach NH_4^+ observations and yield excess NH_3. We believe automotive and wood-smoke sources of NH_3 are more than needed to account for measured NH_4^+/SO_4^{2-} ratio. Results of sensitivity experiments have shown NH_3 could be greater than estimated with no indication present in NH_4^+ observations downtown, possibly yielding enhanced formation of NH_4NO_3 outside of the primarily polluted area.

The origin and chemistry of sulfate aerosol in Fairbanks winter is currently unknown. Emissions used in this simulation, constrained by observations, estimate column integrated total sulfur is in the form of 93% SO_2 and 7% SO_4^{2-}, respectively. A value of 7% is likely too high to be purely primary sulfate emission, but the modeled base case scenario produces no secondary sulfate, which would be expected in an atmosphere with weak photolysis and devoid of oxidants. Sulfur oxidation catalysis by transition metals has been presented as a sulfate formation mechanism (Brandt and van Eldik, 1995) and could be a significant secondary SO_4^{2-} source during winter. If the formation of SO_4^{2-} by metal catalysis is fast, the sulfate could appear like true primary emissions, as

we have modeled them in this study. The fate of NO_x emissions is found to be insensitive to SO_2, but this may not have been the case if secondary sulfate was formed by pathways alternative to photolysis. Additional study would be useful for understanding the sulfate chemistry in Fairbanks and identifying possible remedies for $PM_{2.5}$ non-attainment.

2.6 Conclusions

Simulations have shown approximately two-thirds of NO_x is lost in two days after emission in high-latitude winter conditions through the dark oxidation pathway. Pollution fluxes near the upper limits of observations under high-latitude winter conditions produced a reduced environment with excess NO and depleted O_3. The fraction of emitted NO_x that remains in the atmosphere was found to be most sensitive to NO emission flux and temperature. Winter months with relatively warm temperatures and high mixing heights are likely to have the greatest nitrate aerosol particulate loading. Alternatively, cold days with low mixed layers are likely to have the greatest dry deposition rates and greatest local nitrogen deposition impact. Dry deposition rates of N_2O_5 were found to be most sensitive to aerosol surface area and dry deposition velocity, illustrating the competition between dry deposition and aerosol reactivity for removal of N_2O_5. Due to ground contact only occurring in the bottom model layer, greater amounts of total emitted NO_x were removed from the column via aerosol particle reactions (38%) than through dry deposition (17%) two days after emission in the base case scenario. Modeled abundances of N_2O_5 showed diurnal variations of over 1000% and positive

vertical gradients from the snowpack, showing need for further study to understand vertical distribution of the emission plume and estimate potential impacts.

2.7 Acknowledgements

The authors would like to thank NOAA for use of the Ferret program for analysis of model output and UCAR for the use of NCL plotting software, which was used to generate the figures in this manuscript. The authors would like to thank Deanna Huff, Jim Connor, and Barabara Trost with the Alaska Department of Environmental Conservation for collaboration and providing observational data. Thanks to Catherine Cahill and Tom Trainor for comments and revisions of the manuscript. This project was funded by NSF under grant ATM-0926220.

2.8 References

Akagi, S. K., Yokelson, R. J., Wiedinmyer, C., Alvarado, M. J., Reid, J. S., Karl, T., Crounse, J. D. and Wennberg, P. O.: Emission factors for open and domestic biomass burning for use in atmospheric models, Atmos. Chem. Phys., 11(9), 4039–4072, doi:10.5194/acp-11-4039-2011, 2011.

Alaska Climate Data Center (ACRC). "Fairbanks, AK." <http://climate.gi.alaska.edu/Climate/Location/TimeSeries/Fairbanks.html> Last accessed :10 Oct 2011.

Alaska Department of Environmental Conservation (ADEC). Supplemental Information: $PM_{2.5}$ Designation and Boundary Recommendations. <http://dec.alaska.gov/air/doc/PM25_info.pdf> Dec 2007. Last accessed: 22 Oct 2011.

Alaska Department of Environmental Conservation (ADEC). Fairbanks non-attainment area boundary comments. Emissions inventory 2005. <http://www.dec.state.ak.us/air/doc/DEC_EPA_Fbks_NA_20oct08.pdf> Oct 2008. Last accessed: 22 Oct 2011.

Apodaca, R., Huff, D. and Simpson, W.: The role of ice in N_2O_5 heterogeneous hydrolysis at high latitudes, Atmos. Chem. Phys, 8, 7451–7463, 2008.

Arctic Research of the Composition of the Troposphere by Aircraft and Satellites (ARCTAS). NASA DC-8 aircraft data. <http://www-air.larc.nasa.gov/cgi-bin/arcstat-c> Last accessed: 13 Dec 2011.

Ayers, J. D. and Simpson, W. R.: Measurements of N_2O_5 near Fairbanks, Alaska, J. Geophys. Res, 111(D14), D14309, doi:10.1029/2006JD007070, 2006.

Baum, M. M., Kiyomiya, E. S., Kumar, S., Lappas, A. M. and Lord, H. C.: Multicomponent Remote Sensing of Vehicle Exhaust by Dispersive Absorption Spectroscopy. 1. Effect of Fuel Type and Catalyst Performance, Environ. Sci. Technol., 34(13), 2851–2858, doi:10.1021/es991351k, 2000.

Bertram, T. and Thornton, J.: Toward a general parameterization of N_2O_5 reactivity on aqueous particles: the competing effects of particle liquid water, nitrate and chloride, Atmos. Chem. Phys, 9, 8351–8363, 2009.

Bishop, G. A., Peddle, A. M., Stedman, D. H. and Zhan, T.: On-Road Emission Measurements of Reactive Nitrogen Compounds from Three California Cities, Environ. Sci. Technol., 44(9), 3616–3620, doi:10.1021/es903722p, 2010.

Bott, A. and Trautmann, T.: A numerical model of the cloud-topped planetary boundary-layer: Radiation, turbulence and spectral microphysics in marine stratus, Q. J. R. Meteorol. Soc., 122, 635-667, 1996.

Brandt, C. and van Eldik, R.: Transition metal-catalyzed oxidation of sulfur (IV) oxides. Atmospheric-relevant processes and mechanisms, Chem. Rev., 95, 119-190, 1995.

Brown, S., Stark, H., Ryerson, T., Williams, E., Nicks, D., Trainer, M., Fehsenfeld, F. and Ravishankara, A.: Nitrogen oxides in the nocturnal boundary layer: Simultaneous in situ measurements of NO_3, N_2O_5, NO_2, NO, and O_3, J. Geophys. Res, 108(D9), doi:10.1029/2002JD002917, 2003.

Brown, S., Dubé, W., Osthoff, H., Wolfe, D., Angevine, W. and Ravishankara, A.: High resolution vertical distributions of NO_3 and N_2O_5 through the nocturnal boundary layer, Atmos. Chem. Phys. Disc., 6(5), 9431–9458, 2007a.

Brown, S., Dubé, W., Osthoff, H. and Stutz, J.: Vertical profiles in NO_3 and N_2O_5 measured from an aircraft: Results from the NOAA P-3 and surface platforms during the New England Air Quality Study 2004, J Geophys. Res, 2007b.

Dentener, F. J. and Crutzen, P. J.: Reaction of N_2O_5 on Tropospheric Aerosols: Impact on the Global Distributions of NO_x, O_3, and OH, J. Geophys. Res, 98, 7149-7163, 1993.

Earth System Research Laboratory (ESRL). Global Monitoring Division. Surface ozone, in-situ, hourly averages, Barrow, AK. <http://www.esrl.noaa.gov/gmd/dv/data/index.php?site=brw&category=Ozone&parameter_name=Surface%2BOzone> Last accessed: 15 Oct 2011.

Fenn, M., Baron, J., Allen, E., Rueth, H., Nydick, K., Geiser, L., Bowman, W., Sickman, J., Meixner, T. and Johnson, D.: Ecological effects of nitrogen deposition in the western United States, BioScience, 53(4), 404–420, 2003.

Finlayson-Pitts, B. and Pitts, J.: Chemistry of the Upper and Lower Atmosphere, Academic Press. 2000.

Fochesatto, J., Collins, R., Yue, J., Cahill, C. and Sassen, K.: Compact eye-safe backscatter lidar for aerosol studies in urban polar environment, in Lidar Remote Sensing for Environmental Monitoring VI, vol. 5887, pp. 58870U–58870U–9, SPIE. 2005.

Geyer, A. and Stutz, J.: Vertical profiles of NO_3, N_2O_5, O_3, and NO_x in the nocturnal boundary layer: 2. Model studies on the altitude dependence of composition and chemistry, J. Geophys. Res, 109(D12), D12307, 2004.

Graedel, T. E. and Keene, W. C.: Tropospheric budget of reactive chlorine, Global Biogeochem. Cycles, 9(1), 47, doi:10.1029/94GB03103, 1995.

Hanson, D. R. and Ravishankara, A. R.: The Reaction Probabilities of $ClONO_2$ and N_2O_5 on 40 to 75% Sulfuric Acid Solutions, J. Geophys. Res, 96(D9), 17307–17314, doi:10.1029/91JD01750, 1991.

Huff, D. M., Joyce, P. L., Fochesatto, G. J. and Simpson, W. R.: Deposition of dinitrogen pentoxide, N2O5, to the snowpack at high latitudes, Atmos. Chem. and Phys., 11(10), 4929–4938, doi:10.5194/acp-11-4929-2011, 2011.

Jaenicke, R.: Tropospheric aerosols, Chapter 1: Aerosol-Cloud-Climate Interactions, 1993.

Kean, A. J., Harley, R. A., Littlejohn, D. and Kendall, G. R.: On-Road Measurement of Ammonia and Other Motor Vehicle Exhaust Emissions, Environ. Sci. Technol., 34(17), 3535–3539, doi:10.1021/es991451q, 2000.

National Climate Data Center (NCDC). Relative humidity from station PAFA, 5-min, November 2009. <ftp://ftp.ncdc.noaa.gov/pub/data/asos-fivemin/6401-2009/> Last accessed: 15 Oct 2011.

Osthoff, H., Roberts, J., Ravishankara, A., Williams, E., Lerner, B., Sommariva, R., Bates, T., Coffman, D., Quinn, P., Dibb, J., Stark, H., et al.: High levels of nitryl chloride in the polluted subtropical marine boundary layer, Nature Geoscience, 1, 2008.

Piot, M. and von Glasow, R.: The potential importance of frost flowers, recycling on snow, and open leads for Ozone Depletion Events, Atmos. Chem. and Phys. Disc., 7(2), 4521–4595, 2008.

Seinfeld, J. H. and Pandis, S. N.: Atmospheric Chemistry and Physics, 2nd ed. 2006.

Sommariva, R., Osthoff, H., Brown, S., Bates, T., Baynard, T., Coffman, D., de Gouw, J., Goldan, P., Kuster, W. and Lerner, B.: Radicals in the marine boundary layer during NEAQS 2004: a model study of day-time and night-time sources and sinks, Atmos. Chem. Phys. Disc., 8(4), 16643–16692, 2008.

State of Alaska 2008. Measurements of NO_x and SO_2 from downtown Fairbanks, 2008-2009. Obtained through personal communication with Alaska Department of Environmental Conservation, Jun 2011.

State of Alaska, 2011. Aerosol particle composition data from downtown Fairbanks, 2006-2010. Obtained through personal communication with Alaska Department of Environmental Conservation, May 2011.

Thornton, J. A., Kercher, J. P., Riedel, T. P., Wagner, N. L., Cozic, J., Holloway, J. S., Dubé, W. P., Wolfe, G. M., Quinn, P. K., Middlebrook, A. M., Alexander, B., et al.: A large atomic chlorine source inferred from mid-continental reactive nitrogen chemistry, Nature, 464(7286), 271–274, doi:10.1038/nature08905, 2010.

Total Ozone Mapping Spectrometer (TOMS). What is the total column ozone over your house? <http://toms.gsfc.nasa.gov/teacher/ozone_overhead_v8.html> Accessed: 10 October 2011.

Van Doren, J., Watson, L., Davidovits, P., Worsnop, D., Zahniser, M. and Kolb, C.: Uptake of N_2O_5 and HNO_3 by aqueous sulfuric acid droplets, J. Phys. Chem., 95, 1684-1689, 1991.

von Glasow, R., Sander, R., Bott, A. and Crutzen, P.: Modeling halogen chemistry in the marine boundary layer. 1. Cloud-free MBL, J. Geophys. Res, 107(43418211), 4352, 2002.

Wesely, M.: Parameterization of surface resistances to gaseous dry deposition in regional-scale numerical models, Atmospheric Environment (1967), 23, 1293-1304, 1989.

Wesely, M. and Hicks, B.: A review of the current status of knowledge on dry deposition, Atmospheric Environment, 34(12-14), 2261–2282, 2000.

Wood, E., Bertram, T. and Wooldridge, P.: Measurements of N_2O_5, NO_2, and O_3 east of the San Francisco Bay, Atmos. Chem. Phys., 5, 483-491, 2005.

Yokelson, R. J., Griffith, D. W. T. and Ward, D. E.: Open-path Fourier transform infrared studies of large-scale laboratory biomass fires, J. Geophys. Res, 101(D15), 21067–21080, doi:10.1029/96JD01800, 1996.

Yokelson, R. J., Susott, R., Ward, D. E., Reardon, J. and Griffith, D. W. T.: Emissions from smoldering combustion of biomass measured by open-path Fourier transform infrared spectroscopy, J. Geophys. Res, 102(D15), 18865–18877, doi:10.1029/97JD00852, 1997.

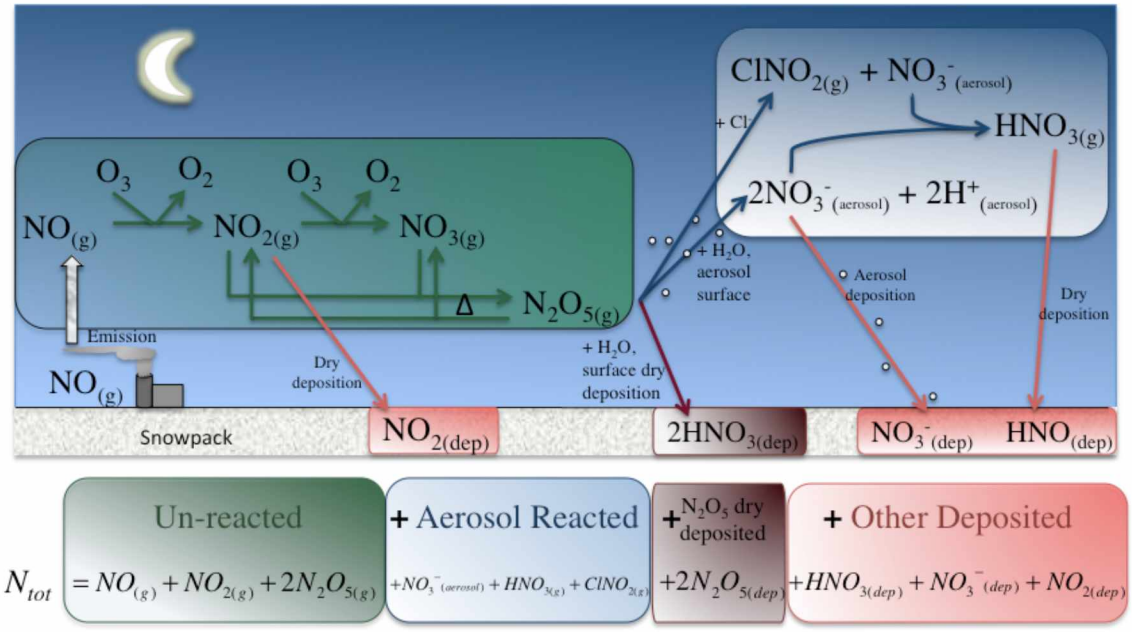

Fig. 2.1: A nocturnal nitrogen schematic with emphasis on N_2O_5 reactivity. The total nitrogen equation (N_{tot}) is a sum of the total column integrated nitrogen from emitted NO_x, divided into speciation fractions.

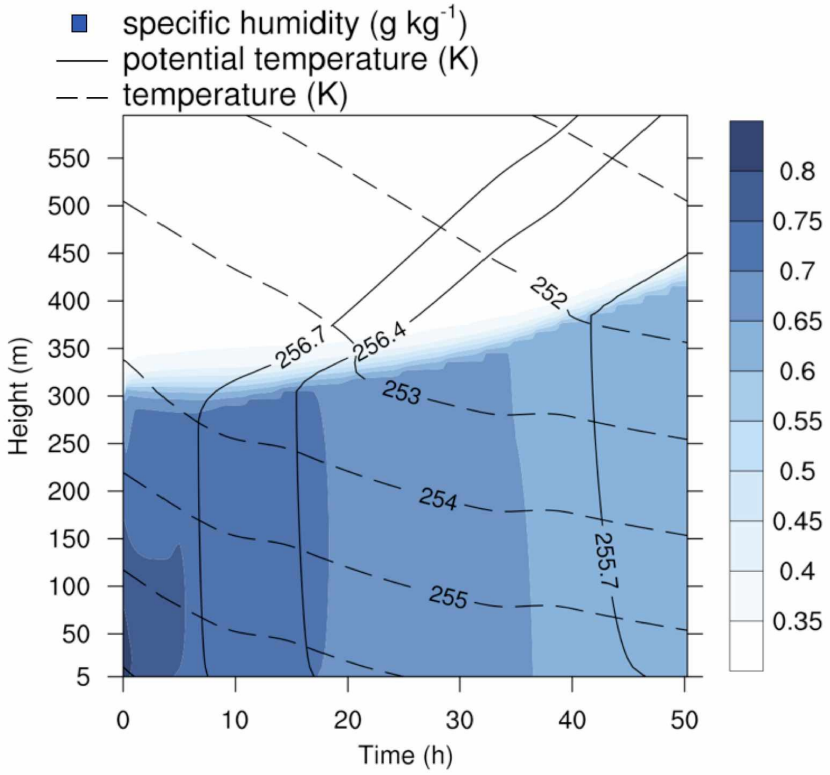

Fig. 2.2: Modeled meteorological parameters include temperature (dashed contours), potential temperature (solid contours), and specific humidity (blue). The modeled mixing height is initialized to be 300 m.

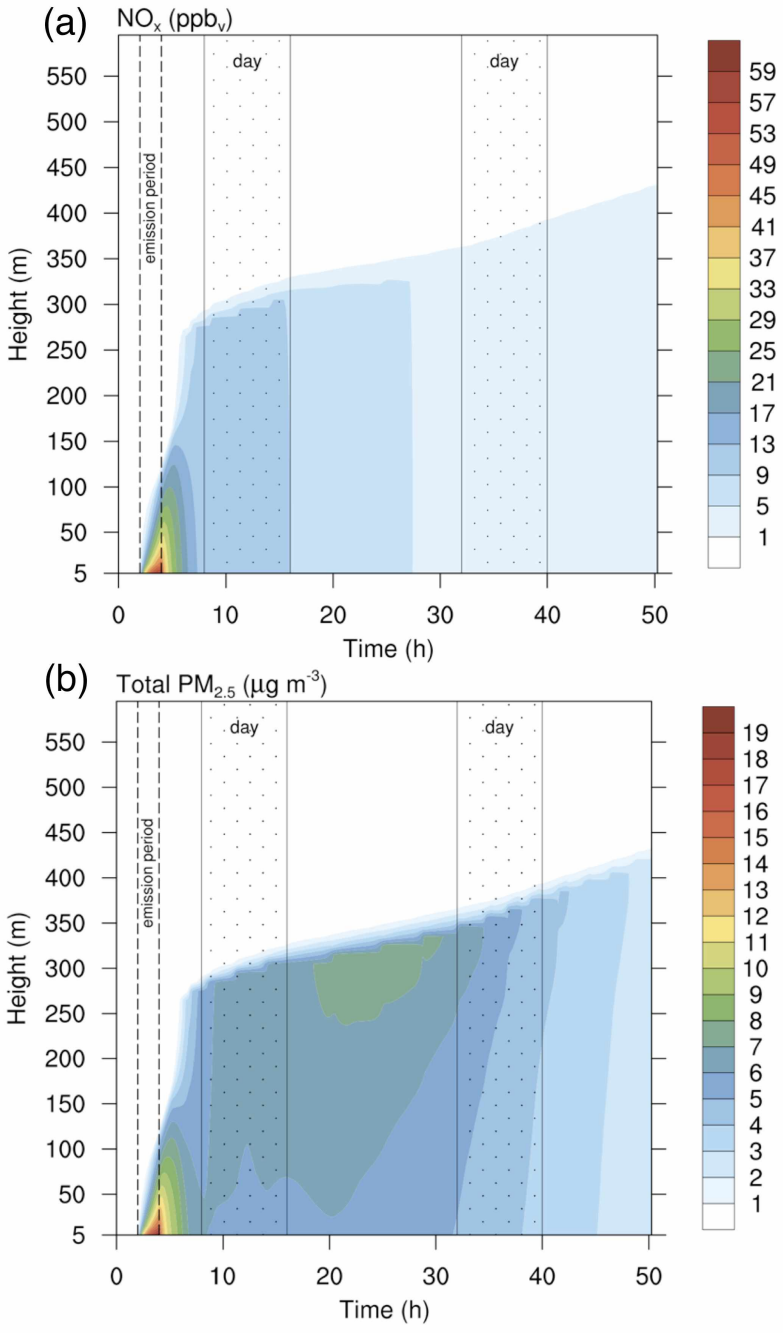

Fig. 2.3: Modeled evolution of primary emission NO_x and total $PM_{2.5}$ begins at local midnight. Daytime regions are indicated by the dotted region and the emission period is indicated by the dotted lines. Emitted species dilute throughout the mixed layer. NO_x undergoes chemical loss (a) while total $PM_{2.5}$ increases (b), primarily due to formation of particulate nitrate.

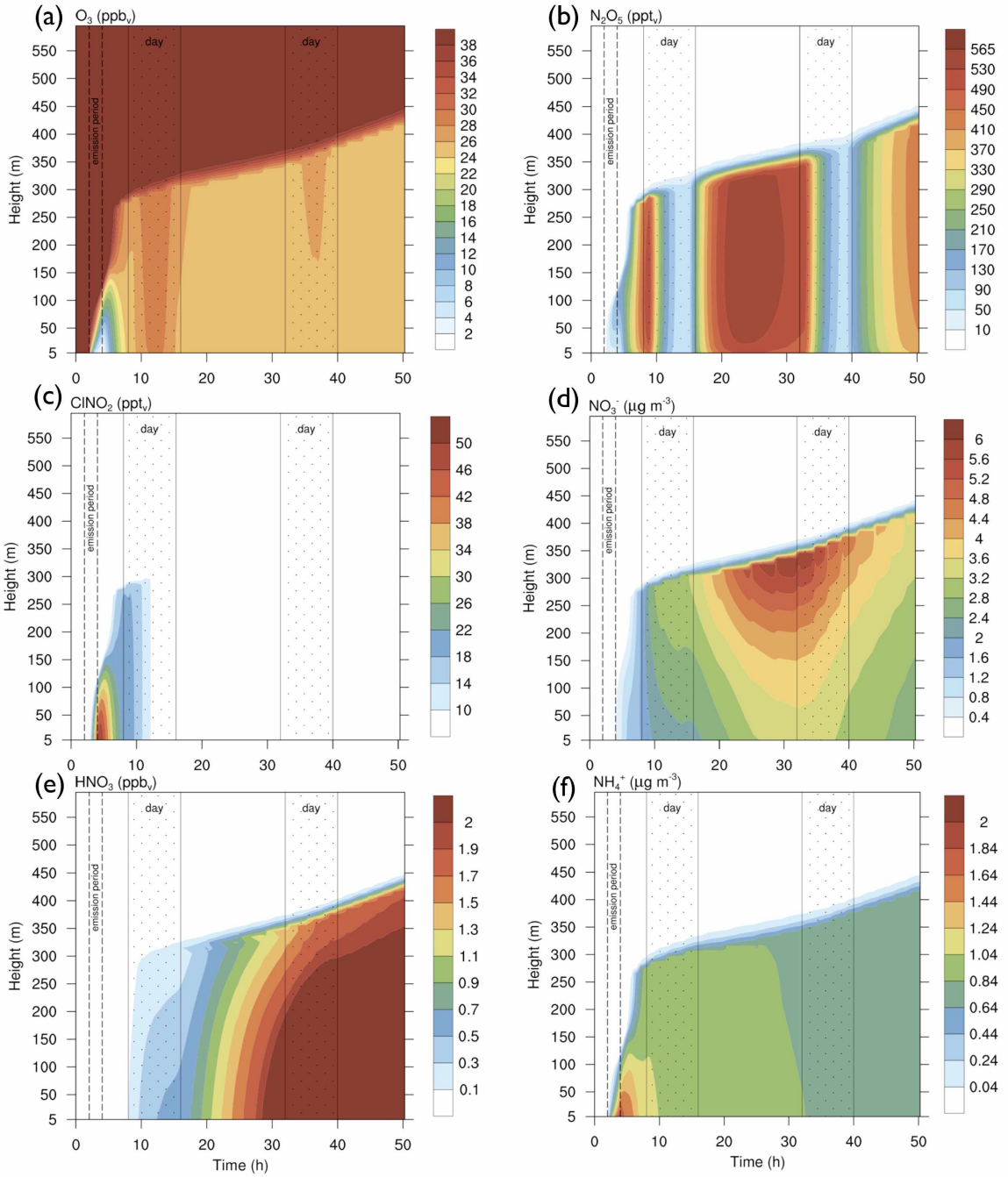

Fig. 2.4: Additional species result from emissions and evolve over time and height above ground level. Modeled NO_3^- and NH_4^+ are total aerosol mass density (sum of all aerosol particle sizes). Daytime regions are indicated by the dotted region and the emission period is indicated by the dotted lines.

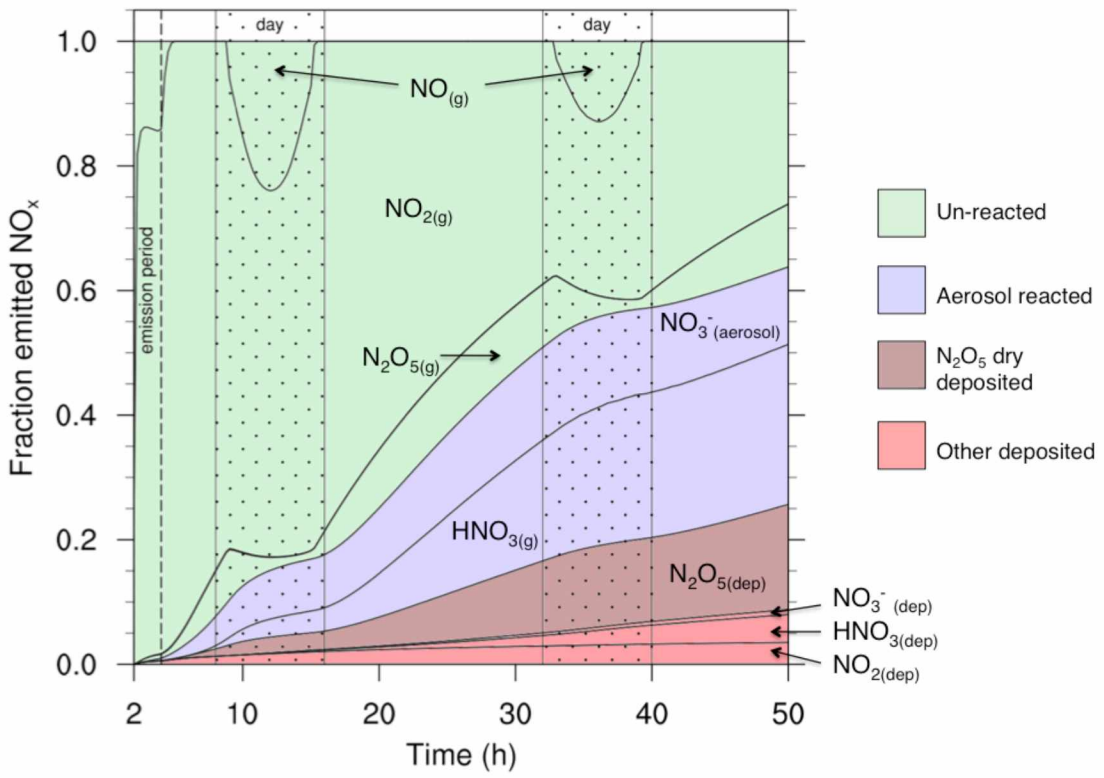

Fig. 2.5: Speciation diagram above shows column integrated chemical loss of NO_x over time. Each section depicts column integrated fraction of labeled species out of total emitted NO_x versus model time, beginning at the start of emission period (t=2 h). Formation of NO and loss of N_2O_5 occur in daylight. Color categories correspond to Fig. 2.1.

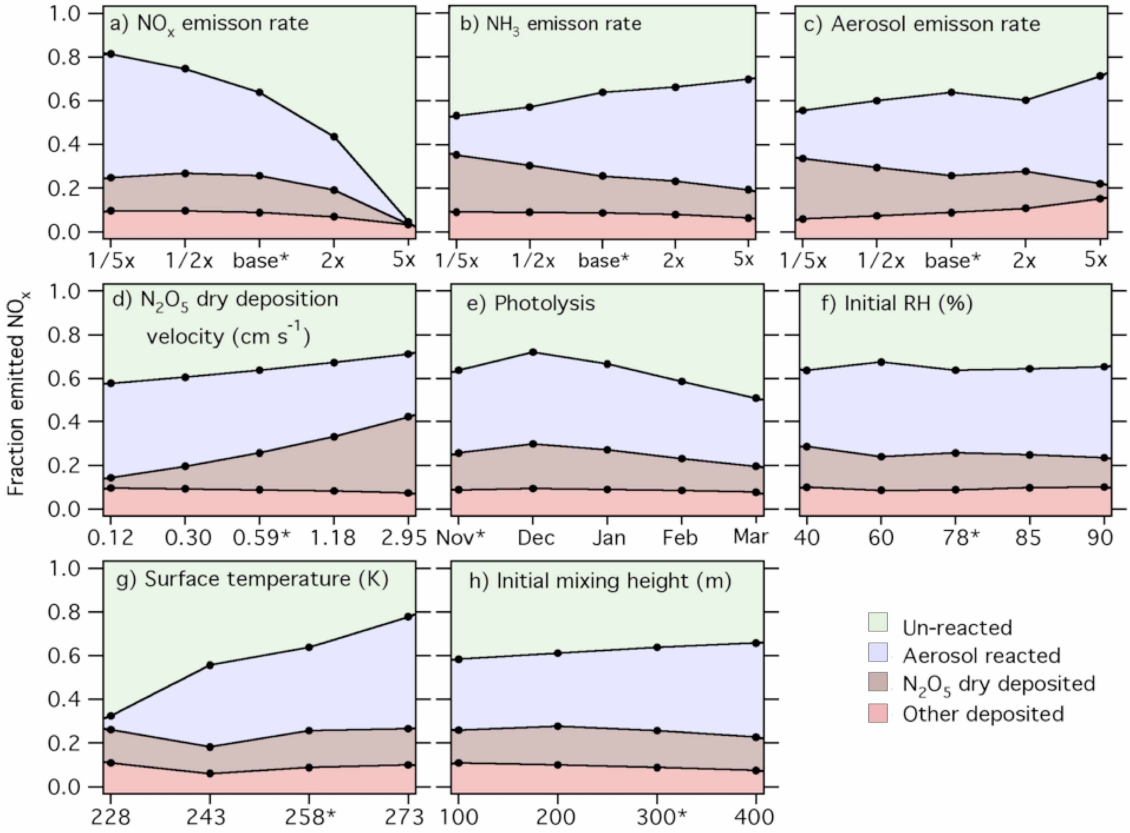

Fig. 2.6: Sensitivity of the fate of emitted NO_x to model parameters was investigated by variations of constraints on the base case. Shown are speciation fractions of total column nitrogen emitted as NO_x at t=50 h, corresponding to two days after the emission period begins. Base case runs are marked by an asterisk (*).

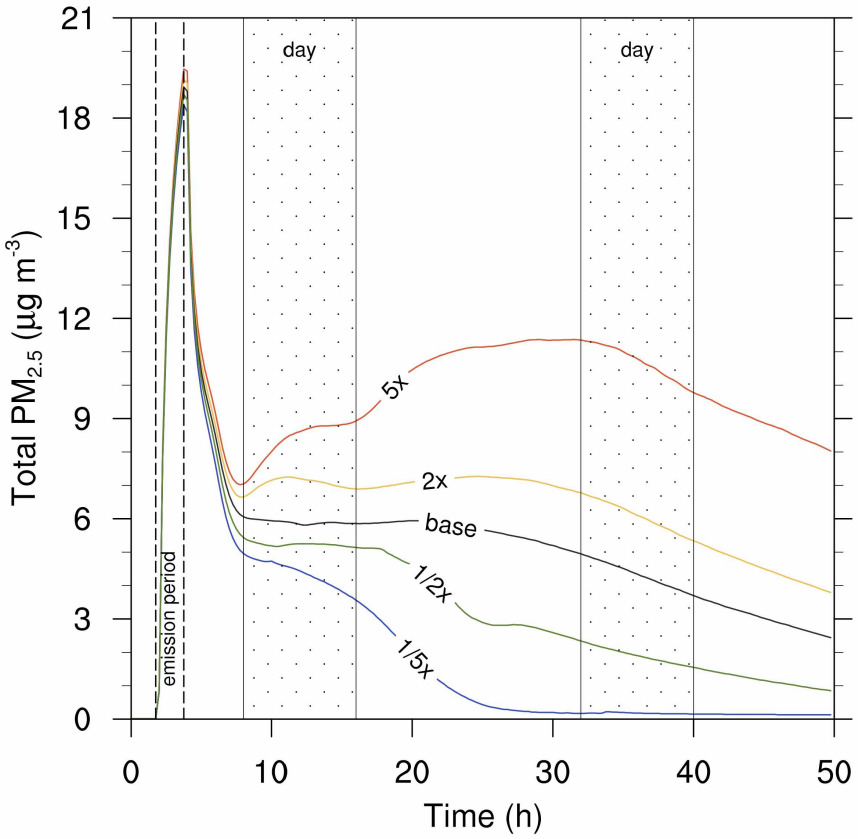

Fig. 2.7: Secondary formation of ammonium nitrate begins at t=8 h and is controlled in magnitude by NH_3 abundance and in time by NO_3^- formation. Pictured above is total $PM_{2.5}$ for the lowest model layer (5m) for each NH_3 sensitivity experiment.

Table 2.1: Observations from downtown Fairbanks were used to constrain the modeled pollution plume at the end of the pollution injection period (t=4 h).

Emission Parameter	Base case 5m, t=4h	Observed Q_1-Q_3 or average	Reference
NO_x (ppb_v)	58	31 - 103	downtown Fairbanks, November 2008 (State of Alaska, 2008)
SO_2 (ppb_v)	12	8.8 - 20.6	downtown Fairbanks, November 2008 (State of Alaska, 2008)
NH_3 (ppb_v)	1.5	-	no known observations
$PM_{2.5}$ ($\mu g\ m^{-3}$)	19	19	downtown Fairbanks, Nov. 2008 average (ADEC, 2007)
$PM_{2.5}$ SO_4^{2-} (% mass)	18%	18%	downtown Fairbanks, Nov. 2008 average (ADEC, 2007)
$PM_{2.5}$ Cl^- (% mass)	0.4%	0.5%	downtown Fairbanks, November average (State of Alaska, 2011)
$PM_{2.5}$ NH_4^+/SO_4^{2-} ($mol\ mol^{-1}$)	1.5	1.5 - 2.4	downtown Fairbanks, annual average (State of Alaska, 2011)

Table 2.2: Field observations of NO_x from downtown Fairbanks, University of Alaska Fairbanks (UAF), and the Quist Farm are used to validate modeled diffusion at ground level. A wind speed of 1 m s^{-1} and distance from downtown was used to calculate corresponding model time.

	Downtown	UAF	Quist Farm
Distance from downtown (km, direction)	0	5, WNW	20, WSW
Corresponding model time (h)	4	5	8
Modeled NO_x (ppb_v)	58	29	12
Observed NO_x range (ppb_v)	1 – 390	0 – 100	0 – 15
Reference	(State of Alaska, 2008)	(Ayers and Simpson, 2006)	(Huff et al., 2011)

Chapter 3: Conclusions and Outlook

3.1 Conclusions

Simulations of an urban pollution plume emitted into a high-latitude winter environment were performed using a 1-D microphysical atmospheric chemistry model. Model results have shown that loss of NO_x through the dark oxidation pathway is an efficient loss mechanism and dominates NO_x loss at high latitudes in winter. Speciation analysis of the evolution of emitted NO_x in time has shown formation of N_2O_5 occurs within hours of emission. Dry deposition of N_2O_5 dominates nitrogen deposition to the snowpack on the local scale near the emission source, while nitrate formed in aerosol particles can remain suspended in the atmosphere until removed by a deposition event such as precipitation. Modeled vertical profiles of N_2O_5 show a positive vertical gradient with peak abundances aloft due to loss of N_2O_5 to the snowpack through dry deposition. Dry deposition of N_2O_5 was found to make up a significant loss mechanism for total emitted NO_x, but N_2O_5 loss to aerosol particles dominates NO_x loss throughout the column due to limited contact with the snowpack in air parcels aloft.

Experiments analyzing the sensitivity of the fate of NO_x to model parameters found that the NO_x flux, photolysis, and temperature are the most important factors controlling chemistry of emitted NO_x. Experiments that assumed NO_x mixing ratios on the upper limits of observations found that sufficient magnitude of emitted NO_x can "titrate" the mixed layer by depleting ozone. This titration effect significantly alters the state of the lower atmosphere by removing oxidants and stopping the dark oxidation

pathway from occurring. Titrated air masses can lead to excess NO and depleted ozone for hours, which will delay the formation of N_2O_5 and lead to deposition impacts further away from the emission source. Simulations of December have shown the dark oxidation pathway of NO_x to be an efficient removal mechanism of NO_x, where the least sunlit conditions yielded the most NO_x removal. Additionally, temperature was found to be one of the most important factors controlling NO_x removal in dark, high-latitude conditions. Extreme cold temperatures hindered kinetic reaction rates, especially heterogeneous chemistry, and led to less NO_x loss.

Sensitivities of ammonium nitrate formation to ammonia flux have suggested that excess ammonia in a polluted area can dictate the magnitude of secondary aerosol particle formation downwind. Ammonium formation can act to neutralize sulfate in the particles and is the only likely secondary aerosol particle formation that occurs in the polluted area due to delay in nitrate formation. Due to the titration effect's timescale limitation on nitrate formation, ammonium nitrate is formed in greatest magnitude outside of the polluted area. Simulations resulted in fairly high concentrations of ammonium nitrate, suggesting fertilization of ecosystems downwind may occur due to NO_x emissions.

3.2 Future outlook

Additional sensitivity experiments may be performed to analyze model sensitivities to two parameters varied at the same time. Ideally, parameters that may be coupled together in the observable atmosphere would be varied, such as NO emission

flux and aerosol particle emission rate, and mixed height and temperature. Experiments where more than one parameter is varied may produce insightful results. For example, Fig. 2.6c shows an unexpected result where the 2x aerosol particle emission rate experiment results in a decreased aerosol reacted fraction. Many experiments were performed to analyze the cause of this result. No explanation was found, but an experiment where the aerosol particle emission flux was varied over 1/2x the base case NO emission flux yielded the expected result of a linear relationship between aerosol particle emission flux and the aerosol reacted fraction. This suggests a relationship between NO emission flux and aerosol particle surface area that may require further study.

Results from this study suggest that measurements of N_2O_5 be performed from aircraft to gain a better understanding of the magnitude and spatial distribution of nocturnal nitrogen species. Aircraft measurements would confirm whether loss to the snowpack, building, or tree surfaces was affecting measurements. The fate of emitted NO_x could be tracked in time using transects leading downwind from the emission source, which could be compared to model results from this study.

It is likely that dry deposition of N_2O_5 is underestimated in this study. The greater Fairbanks area is surrounded by black and white spruce, birch, aspen, and willow. Measured dry deposition velocity of N_2O_5 used to constrain the model was collected over a flat, foliage-free surface, and the model did not account for loss of N_2O_5 to trees. Sensitivity experiments investigating the role of trees in the dry deposition equation found the model parameterization increased dry deposition velocities of HNO_3 by 12%

with the addition of an upper canopy into the equation. Despite this increase in deposition, modeled N_2O_5 abundances near the ground are near double observed values, suggesting loss of N_2O_5 near the ground is not sufficiently captured. For this reason, experiments to determine the amount of N_2O_5 lost to foliage, especially snow covered foliage, may prove useful in understanding the fate of NO_x. This would require micrometeorological measurements of three-dimensional wind speeds and simultaneous high frequency N_2O_5 measurements at different heights above the snowpack in and above a forested area. Enhanced dry deposition of N_2O_5 on the tree surfaces themselves is unlikely at temperatures well below 273 K, but snow-covered trees often compose a complex, three-dimensional lattice of surface area covered by snow on which enhanced dry deposition may occur.

Field studies similar to Ayers and Simpson (2006), Apodaca et al. (2008) and Huff et al. (2011) may be performed downwind of Barrow, Alaska or Deadhorse, Alaska to determine the effect of particulate chloride concentrations on the fate of emitted NO_x. It would be useful to include measurements of $ClNO_2$ in such an experiment. Similar to Mielke et al. (2011), a suite of measurements including NO, NO_2, O_3, N_2O_5, $ClNO_2$, and aerosol speciation should be performed. Results may suggest high abundance of $ClNO_2$ leading to significant chloride activation downwind, especially in polar springtime.

Additionally, such a field project as explained above could be used to constrain MISTRA for additional analysis. Model studies would allow for analysis of chemical species far downwind, beyond the reach of reasonable instrumental analysis, and investigate the fate of nitrogen pollution under maritime-polar conditions. More

importantly, modeling results may find that chlorine activation by $ClNO_2$ plays a key role in ozone depletion events in polar springtime outside of the observed area. Supplemental observations of bromine species coupled with $ClNO_2$ and N_2O_5 observations would be necessary to investigate this possible mechanism of ozone depletion event initiation. A result finding chloride activation by $ClNO_2$ would imply that anthropogenic NO_x pollution instigates the ozone depletion events and is responsible for the subsequent ozone depletion and mercury deposition.

3.3 References

Ayers, J. D. and Simpson, W. R.: Measurements of N_2O_5 near Fairbanks, Alaska, J. Geophys. Res, 111(D14), D14309–, doi:10.1029/2006JD007070, 2006.

Apodaca, R., Huff, D. and Simpson, W.: The role of ice in N_2O_5 heterogeneous hydrolysis at high latitudes, Atmos. Chem. Phys, 8, 7451–7463, 2008.

Huff, D. M., Joyce, P. L., Fochesatto, G. J. and Simpson, W. R.: Deposition of dinitrogen pentoxide, N_2O_5, to the snowpack at high latitudes, Atmos. Chem. Phys., 11(10), 4929–4938, doi:10.5194/acp-11-4929-2011, 2011.

Mielke, L., Furgeson, A. and Osthoff, H.: Observation of $ClNO_2$ in a mid-continental urban environment, Environ. Sci. Technol., doi:10.1021/es201955u, 2011.

Appendix A: Simulations of emissions from Barrow, AK in winter and spring

A.1 Introduction

Emissions of NO_x in the North Slope Borough of Alaska contribute heavily to total NO_x emissions in the state due to resource extraction and extreme living environments requiring increased power consumption. In 2002, NO_x emissions from the North Slope Borough were greater than the Municipality of Anchorage and the Fairbanks North Star Borough combined (ADEC, 2011), primarily due to point sources. Additionally, a location such as Barrow, AK (71.29°N) will go approximately a month in the winter with no direct sunlight, making for a unique chemical environment. Prevailing ENE winds from the Arctic Ocean (ACRC, 2011) bring a maritime polar aerosol particle distribution rich in halogen species to the urban areas on the coast. Simulations of NO_x emissions from Fairbanks showed a very small sensitivity of the fate of NO_x on chloride (Cl^-) at observed continental aerosol particle concentrations (Chapter 2.4), but did show that Cl^- was able to affect N_2O_5 reactivity on aerosol particles. Base case simulations for Fairbanks formed abundances of 50 ppt_v nitryl chloride ($ClNO_2$). This has prompted investigations into reactivity when greater amounts of Cl^- are present.

One pathway by which "chlorine activation" can occur is ionic particle chloride reacting to form $ClNO_2$, which can then be photolyzed to form NO_2 and chlorine (Cl) radical in the atmosphere. Chlorine radical is highly reactive and can affect O_3 abundance. Halogen activation plays a strong role in ozone depletion events observed in

polar springtime (Foster et al., 2001; Simpson et al., 2007), but not all radical sources are accounted for. For this reason, MISTRA was initialized by parameters to represent an Arctic air mass, rich in Cl^-, passing over Barrow, Alaska to analyze chlorine production. Two experiments, once in December and one in March, are presented to analyze the dependence of chlorine activation on photolysis.

A.2 Model constraints

The Barrow runs were adapted from the base case Fairbanks scenario. The most significant changes to meteorology include Barrow's latitude (71.29°N) and an increase in geostrophic wind speed. Geostrophic wind speed in the model is a theoretical wind speed since it is a 1-D simulation, but is used for turbulence calculations. A greater wind speed will result in faster dilution through the mixed layer. Background aerosol particles were initialized using a tri-modal maritime distribution and composition was constrained by observations described in (Quinn et al., 2002) and available courtesy of NOAA (NOAA, 2011). Field observations of aerosol particles in Barrow are obtained upwind and to the north of the populated area, so particle composition was constrained to the start of the emission period (t=2 h). Table 1 shows comparison of modeled sub-micron and super-micron observations to modeled aerosol bin 1 (sub-micron, dry aerosol particle) and bin 2 (super-micron, dry aerosol). Most important to note is the initialization of 0.4 ug m^{-3} Cl^- throughout the mixed layer in bin 1.

The pollution emission consisted only of NO_x from t=2 h to t=4 h; no NH_3, SO_2, or urban aerosol was emitted from the surface. The magnitude of geographical area of

Barrow and downtown Fairbanks are fairly similar and, despite a much smaller population, is it expected that NO_x emissions are on the same order of magnitude due to home heating and power consumption in winter.

A.3 Results

The experiments for the months of December and March received the same NO_x emission and differed only in photolysis rates corresponding to 21 December and 21 March 21, respectively. The December run received no direct sunlight while the March run received 13 hours of sun per day with photolysis intensity peaking mid-day.

In the December case, NO_x (Fig. A.1a) dilutes rapidly to a height of 175 m at the end of the emission period (t=4 h). Ozone (Fig. A.1b) is reduced to < 2 ppb_v at t=4 h and is less than background ozone for the remainder of the model run. Increases of 2-4 ppb_v in O_3 occur due to entrainment from layers aloft. Under completely dark conditions, N_2O_5 formation (Fig. A.1c) is unhindered from the time of NO_x emission and reaches a maximum value aloft, 12 hours after emission ends. Due to background Cl^- aerosol in the entire mixed layer, $ClNO_2$ forms throughout the mixed layer (Fig. A.1d) upon formation of N_2O_5. No chemical loss of $ClNO_2$ is seen in the model output in the December run. Nitrate aerosol is formed by both heterogeneous hydrolysis of N_2O_5 and reaction to form $ClNO_2$, leading to a significant amount of NO_3^- formation (Fig. A.1e) after the emission period. The lack of photolysis made for essentially zero Cl radical formation (Fig. A.1f) and is presented for comparison purposes.

In the March case, NO_x (Fig. A.2a) dilutes rapidly to 175 m at the end of the emission period (t=4 h). Ozone is reduced to < 2 ppb_v at t=4 h but is recovers during the day to near background levels (Fig. A.2b). Ozone increases during the day because NO_x is repartitioned from its nighttime state of entirely NO_2 to a mixture of NO and NO_2 due to photolysis of NO_2, which produces one molecule of O_3 for each NO_2 photolyzed. Due to fairly intense photolysis, N_2O_5 shows a strong diurnal cycle because it is only produced at night (Fig. A.2c). Mixing ratio of N_2O_5 peaks aloft, but at the end of the second night after sufficient time form in darkness and correlates to the most intense NO_3^- formation (Fig. A.2e). Abundance of $ClNO_2$ peaks just after peak N_2O_5 formation, and is depleted by photolysis by the end of the day (Fig. A.2d). This chemical loss of $ClNO_2$ makes for production of Cl radical in concentrations of $1x10^5$ molecules cm^{-3} in the mixed layer. Peak concentrations of Cl radical follow destruction of $ClNO_2$ during the day and Cl radical production ceases once $ClNO_2$ is depleted.

A.4 Discussion

NO_x emissions into a completely dark environment allow the dark oxidation pathway to carry out un-hindered. This leads to a general build-up of secondary pollutants and losses of $ClNO_2$ only due to dilution, suggesting pollutants formed by such dark mechanisms in winter are carried to more southerly regions where reactions will then take place.

The March simulation highlights the importance of photolysis on N_2O_5 chemistry and chlorine activation. After emission, NO_x is removed less efficiently in the presence of

sunlight (Fig. A.2a). Photolysis in the March run reduces the amount of ozone depletion by production of ozone in the mixed layer from reformation of NO from photolysis of NO_2. The difference in time of peak N_2O_5 formation between December (Fig. A.1c) and March (Fig. A.2c) runs shows how daylight hours can delay formation of N_2O_5, but N_2O_5 peaks in both runs occur approximately after 8 h of darkness. In total darkness, N_2O_5 forms in greater abundance than when formed after a day due to vertical dilution of the source species, NO_x. In the December run, $ClNO_2$ is a reservoir of NO_x and chlorine, but in the March run $ClNO_2$ is readily photolyzed (Fig. A.2d) and is a source of Cl radical on a daily timescale. Additionally, the March simulation forms less NO_3^- than December, as less $ClNO_2$ is produced.

The March run produced peak column densities of 4.5×10^9 molecules Cl cm^{-2}. Figure A.3 compares total column production of Cl^- in the March run to the base case Fairbanks simulation. Through the $ClNO_2$ pathway, concentrations of Cl^- in aerosol particles control chlorine activation in the presence of NO_x and sunlight.

The fate of NO_x in the base case Fairbanks run compared fairly well with the Barrow simulation in March (Fig. A.4). Formation of $ClNO_2$ produces one NO_3^- for each molecule of N_2O_5 destroyed, and photolysis of $ClNO_2$ reforms NO_x. In this manner, NO_x may be recycled through this process while activating chloride and having only a minor effect on the fate of NO_x.

A.5 References

Alaska Climate Research Center (ACRC), 2011. "Monthly wind direction frequency – Barrow" <http://climate.gi.alaska.edu/Climate/Wind/Direction/Barrow/Month.html> Last accessed: 22 Oct 2011.

Alaska Department of Environmental Conservation (ADEC). Amendments to state air quality Control plan. Volume III: Appendix III.K.5. <http://www.dec.state.ak.us/air/anpms/rh/rhdoc2/Appendix%20III.K.5.pdf> 11 Feb 2011. Last accessed: 22 Oct 2011.

Foster, K., Plastridge, R., Bottenheim, J., Shepson, P., Finlayson-Pitts, B. and Spicer, C.: The role of Br_2 and BrCl in surface ozone destruction at polar sunrise, Science, 291(5503), 471, 2001.

National Oceanic and Atmospheric Administration (NOAA), 2011. "NOAA regional aerosol sampling stations." BRW 1997. <http://saga.pmel.noaa.gov/data/stations/> Last accessed: 22 Oct 2011.

Quinn, P., Miller, T., Bates, T., Ogren, J., Andrews, E. and Shaw, G.: A 3-year record of simultaneously measured aerosol chemical and optical properties at Barrow, Alaska, J. Geophysical Res., 107, 4130, 2002.

Simpson, W. R., von Glasow, R., Riedel, K., Anderson, P., Ariya, P., Bottenheim, J., Burrows, J., Carpenter, L. J., Frieß, U., Goodsite, M. E., Heard, D., Hutterli, M., Jacobi, H.-W., Kaleschke, L., Neff, B., Plane, J., Platt, U., Richter, A., Roscoe, H., Sander, R., Shepson, P., Sodeau, J., Steffen, A., Wagner, T., and Wolff, E.: Halogens and their role in polar boundary-layer ozone depletion, Atmos. Chem. Phys., 7, 4375-4418, doi:10.5194/acp-7-4375-2007, 2007

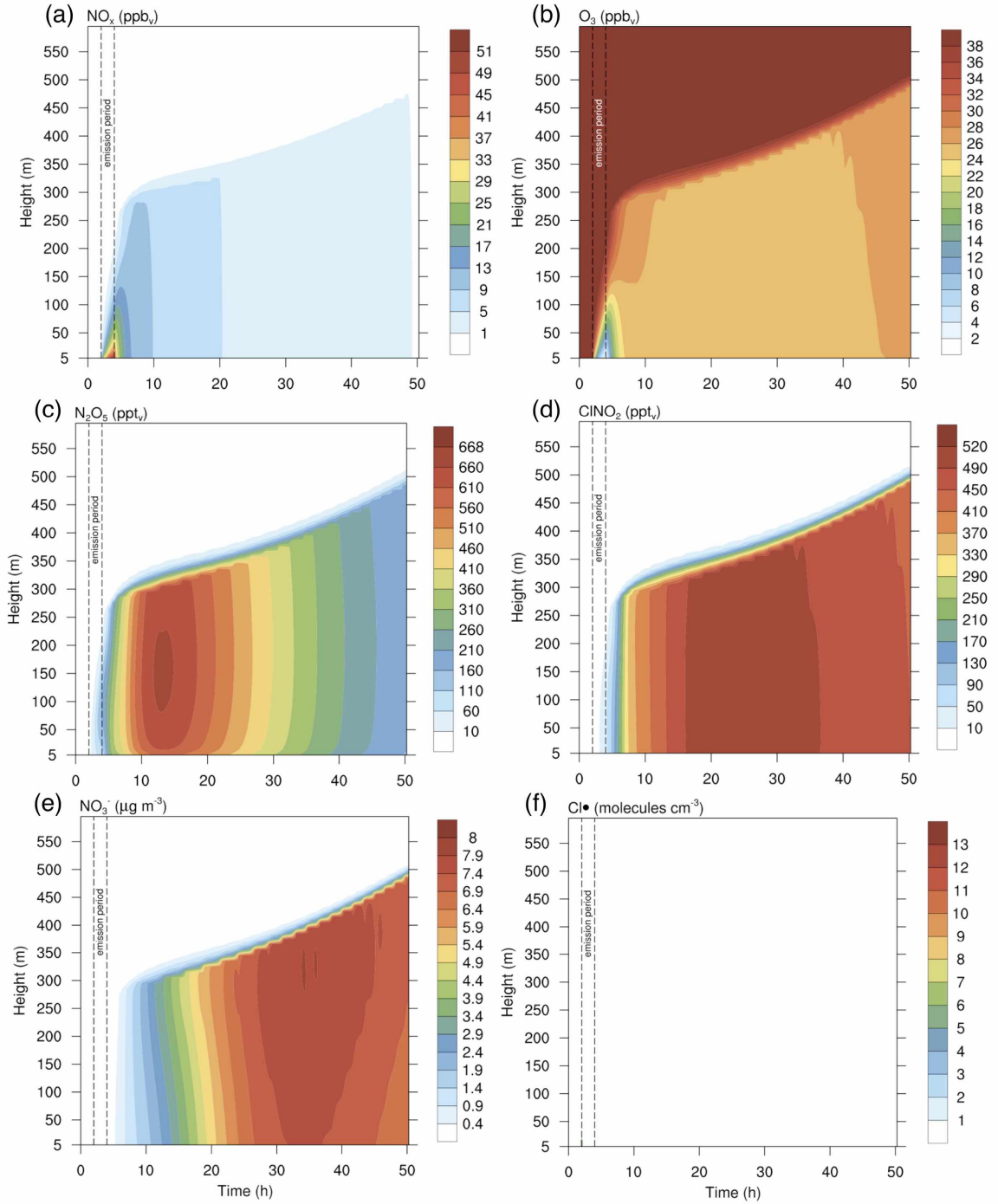

Fig. A.1: With no direct sunlight in December, nocturnal nitrogen species N_2O_5 and $ClNO_2$ form in high abundance but no chlorine radical is produced. The emission period is indicated by the dotted lines.

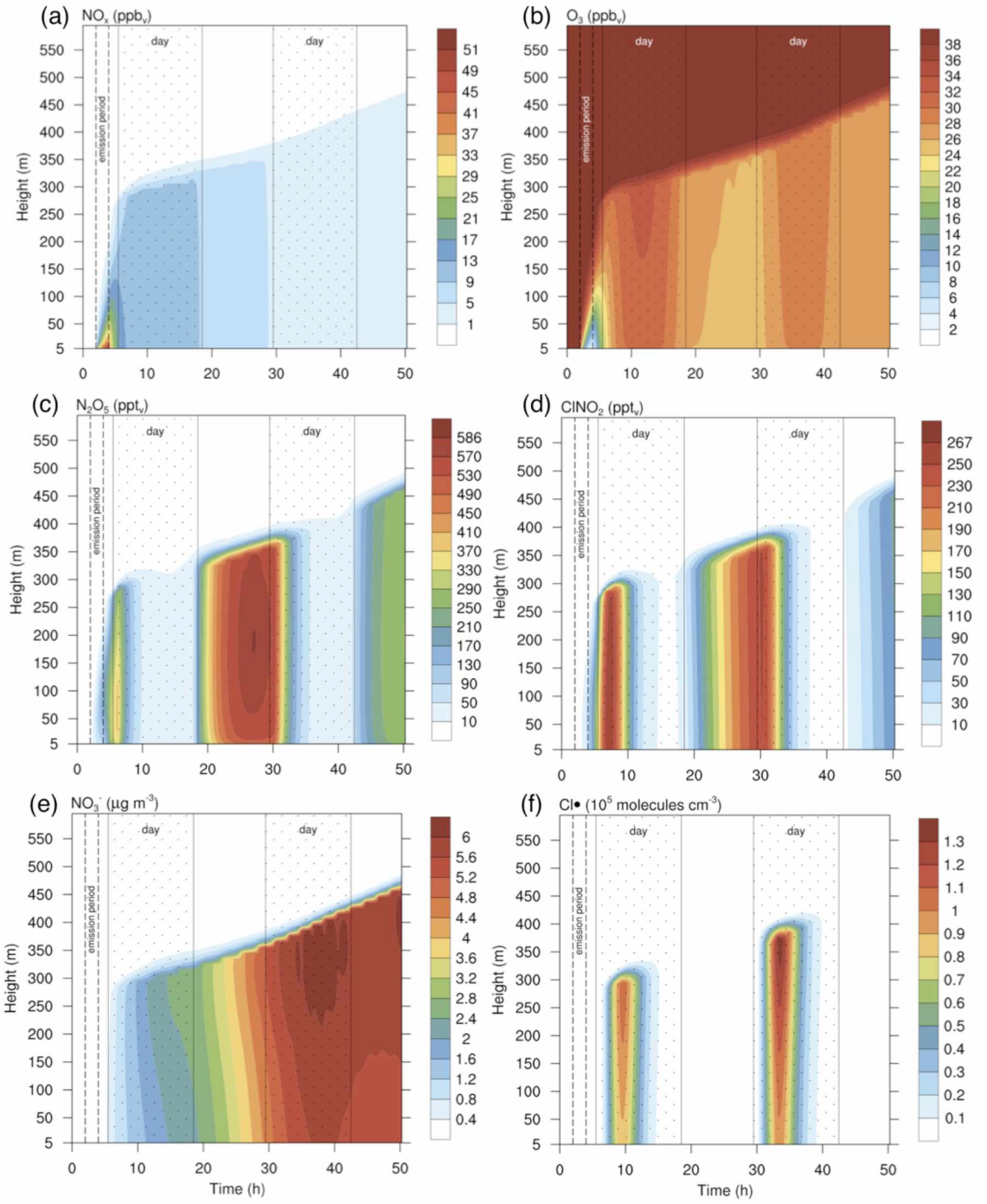

Fig. A.2: In the presence of sunlight in March, N_2O_5 is nearly depleted during daylight hours and photolysis of $ClNO_2$ produces Cl radical in concentrations greater than $1x10^5$ molecules cm^{-3}. Daytime regions are indicated by the dotted region and the emission period is indicated by the dotted lines.

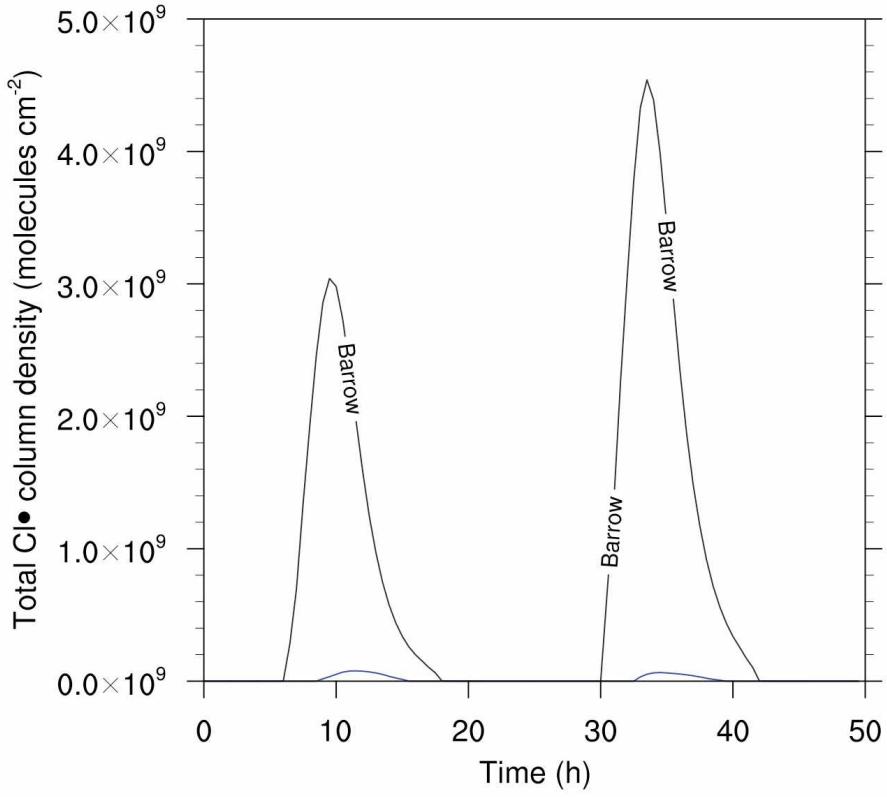

Fig. A.3: Column integrated production of Cl radical in molecules cm^{-2} for Barrow in March (black) and the Fairbanks base case simulation (blue) shows the dependence of chlorine activation on particle Cl^- concentrations.

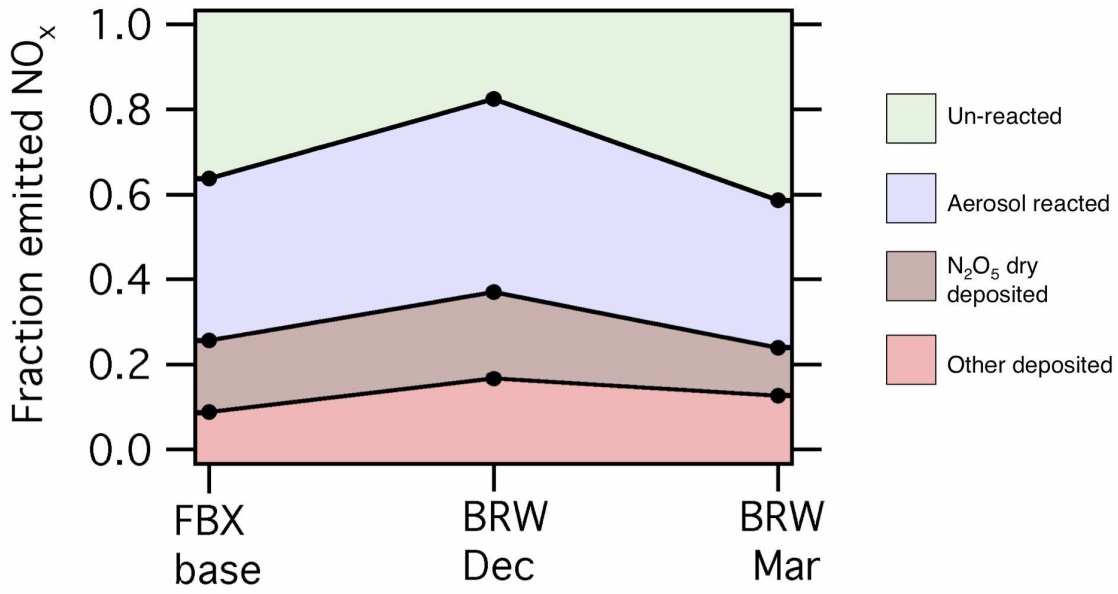

Fig. A.4: Speciation plots similar to those presented in Fig. 2.6 show the fate of NO_x at t=50 h is similar between the Fairbanks (FBX) base case (November) and Barrow (BRW) in March, despite chlorine activation.

Table A.1: Aerosol particle composition was constrained at t=2 h, before the emission period, to observations at Barrow, AK which were obtained just north and upwind of the populated area.

Species ($\mu g\ m^{-3}$)	Modeled bin 1 (sub-micron) t=2 h	Observed sub-micron March 2008 average	Modeled bin 2 (super-micron) t=2 h	Observed super-micron Annual average
Na^+	0.1	0.3	0.2	0.2
Cl^-	0.4	0.5	0.4	0.3
NH_4^+	0.2	0.2	0.0	0.0
SO_4^{2-}	0.7	0.8	0.0	0.1
NO_3^-	0.0	0.1	0.0	0.0
Organic matter	2.2	-	1.5	-
Total	3.6	3.8	2.1	2.1